SEDS-Proceedings of the 9th GRS Workshop

Safety of Extended Dry Storage of Spent Nuclear Fuel

Garching,
20th – 22nd May 2025

GRS - 845

Gesellschaft für Anlagen-
und Reaktorsicherheit
(GRS) gGmbH

SEDS-Proceedings of the 9th GRS Workshop

Safety of Extended Dry Storage of Spent Nuclear Fuel

Garching, 20th – 22nd May 2025

Oliver Bartos
Florian Rowold
Klemens Hummelsheim

November 2025

Remark:

This report refers to in-house project 4724E03235 which has been funded by the German Federal Ministry for the Environment, Climate Action, Nature Conservation and Nuclear Safety (BMUKN).

The work was conducted by GRS.
The responsibility for the content of the report lies with the authors.

GRS - 845
ISBN 978-3-911727-38-9

Keywords
ageing management, cladding, dry storage, inventory, Safety of the extended dry storage of spent nuclear fuel, SEDS 2025, spent fuel

Introduction

All countries with nuclear power plants do not currently have a repository for high-level radioactive waste in operation. This means that in most countries there is a need to store radioactive waste, such as spent fuel, for longer than planned.

The Safety of Extended Dry Storage of Spent Nuclear Fuel (SEDS) workshop was launched in 2017 as a small, focused conference on progress in the safety aspects of extended dry storage of spent nuclear fuel. The aim is to identify knowledge gaps for extended storage and to exchange ideas with research and expert organisations mainly from Germany, the EU and Switzerland. In 2019, the SEDS workshop gained international recognition as an affiliate of the EPRI-ESCP meeting. Since then, the workshop has become an important event in the international field of extended storage. During the COVID-19 pandemic, the workshop was also held in digital form in 2020 and 2021 with about 100 participants. From a scientific point of view, numerous research topics emerged from the exchange at the SEDS workshop, which also led to new collaborations. It was possible to identify existing knowledge gaps for safe extended storage and to define corresponding research areas.

The Gesellschaft für Anlagen- und Reaktorsicherheit (GRS) gGmbH hosts its 9th SEDS workshop in Garching near Munich on 20th – 22nd May 2025. The event attracted great attention as the program was filled with 20 presentations from 16 institutes and attended by 61 experts from 8 countries. A wide variety of experts was represented at the event, including those from universities and research organisations, technical support organisations, fuel suppliers and authorities.

Content

1 Agenda

SEDS 2025 - 9th Workshop on the
Safety of Extended Dry Storage of Spent Nuclear Fuel

May 20 – 22, 2025 hosted by
Gesellschaft für Anlagen- und Reaktorsicherheit (GRS) gGmbH

Tuesday, May 20

Time	Title	Speaker/ Organization
12:00	Snacks & Drinks	
13:00	Welcoming and Workshop Overview	Chairs
13:20	Evaluation of load scenarios for Spent Fuel Assemblies	K. Simbruner, GRS
13:50	The impact of cooling rate and hydrogen concentration on hydride morphology in Zircaloy-4	P. Kaufholz, BGZ
14:20	Coffee break	
14:40	Mechanical Properties of Irradiated Zircaloy Cladding and Their Impact on Structural Integrity During Dry Interim Storage	T. Lin, KIT
15:10	New results in the framework of the SPIZWURZ project	S. Weick, KIT
15:40	Coffee Break	
16:10	SPIZWURZ Blind Benchmark	A. Rezchikova, GRS
16:40	Modelling hydride re-distribution and re-orientation in DX cladding	M. Zemek, Axpo
17:10	Coffee Break & End of Session	
18:00	Buffet @ GRS in Garching	

Wednesday, May 21

Time	Title	Speaker/ Organization
09:00	Coffee & Tea	
09:30	CIEMAT´s HYDCLAD tool. Contribution to SPIZWURZ Benchmark	F. Feria, CIEMAT
10:00	Framatome's performance in SPIZWURZ creep benchmark	R. Sedlacek, Framatome
10:30	Coffee Break	
11:00	Numerical Investigations on Gd-Burnout of Fuel Assemblies with Low Burnup	V. Hannstein, BGZ
11:30	Calculation of Activation Products of the Structural Components of a Light Water Reactor (LWR) Spent Fuel Assembly using FISPACT-II	R. Narang, TUM

12:00	Lunch Break @ GRS in Garching	
13:00	Research at PSI in respect to intermediate dry storage - current work and outlook	J. Bertsch, PSI
13:30	Impact of the Wet-to-Dry-to-Wet fuel transfer on dry storage	P. Konarski, PSI
14:00	Coffee Break	
14:30	Spent Fuel Integrity, regulator´s perspective and activities in Switzerland	J. Dus, ENSI
15:00	Extended Storage of Spent Nuclear Fuel in Casks - recent developments at TÜV NORD	G. Spykman, TÜV Nord
15:30	Coffee Break	
16:00	Spent fuel storage in Dukovany NPP	J. Gerza & D. Kral, NPP Dukovany
16:30	60 years experience of dry storage of metallic uranium research reactor fuel	P. Bennett, NND
17:00	Coffee Break & End of Session	
19:00	Dinner @ Hofbräukeller in München	

Thursday, May 22

Time	Title	Speaker/ Organization
09:00	Coffee & Tea	
09:30	Generic cask modelling options to promote both exchange and comparability and their illustration using a muographic application	T. Braunroth, GRS
10:00	Non-invasive imaging of transport and storage casks	M. Wagner, HZDR
10:30	Coffee Break	
11:00	On the Applicability of the Master Curve Concept for Ductile Cast Iron based on experimental and microstructural results	M. Holzwarth, US
11:30	Adaptive Service Life Management for Concrete Building Structures of Interim Nuclear Storage Facilities	S. von Wehren, TU-BS
12:00	Summary and Discussion of the Workshop	All
12:30	End of Workshop	

2 Titles of the Lectures of the Authors

1. Evaluation of Load Scenarios for Spent Fuel Assemblies, Kai Simbruner, Gesellschaft für Anlagen – und Reaktorsicherheit (GRS) gGmbH, Germany
2. The Impact of Cooling Rate and Hydrogen Concentration on Hydride Morphology in Zircaloy-4, Peter Kaufholz, Gesellschaft für Zwischenlagerung (BGZ), Germany
3. Mechanical Properties of Irradiated Zircaloy Cladding and Their Impact on Structural Integrity During Dry Interim Storage, Tzu Yen (Yvonne) Lin, Karlsruhe Institute of Technology (KIT), Germany
4. New Results in the Framework of the SPIZWURZ Project, S. Weick, Karlsruhe Institute of Technology (KIT), Germany
5. SPIZWURZ Blind Benchmark, Aleksandra Rezchikova, Gesellschaft für Anlagen – und Reaktorsicherheit (GRS) gGmbH, Germany
6. Modelling Hydride Re-distribution and Re-orientation in DX Cladding, Martin Zemek, Axpo Power AG, Germany
7. CIEMAT´s HYDCLAD Tool - Contribution to SPIZWURZ Benchmark, Francisco Feria, CIEMAT, Spain
8. Framatome's Performance in SPIZWURZ Creep Benchmark, Radan Sedlacek, Framatome, Germany
9. Numerical Investigations on Gd-Burnout of Fuel Assemblies with Low Burnup, Volker Hannstein, Gesellschaft für Zwischenlagerung (BGZ), Germany
10. Calculation of Activation Products of the Structural Components of a Light Water Reactor (LWR) Spent Fuel Assembly using FISPACT-II, Rahul Narang, Technical University of Munich (TUM), Germany
11. Research at PSI in Respect to Intermediate Dry Storage - Current Work and Outlook, Johannes Bertsch, Paul Scherrer Institut (PSI), Schweiz
12. Fuel Performance Modelling of Used Nuclear Fuel Transfer between Storage Pools, Piotr Konarski, Paul Scherrer Institut (PSI), Schweiz
13. Spent Fuel Integrity, Regulator´s Perspective and Activities in Switzerland, Jiri Dus, Eidgenössisches Nuklearsicherheitsinspektorat (ENSI), Schweiz
14. Extended Storage of Spent Nuclear Fuel in Casks - Recent Developments at TÜV NORD, Gerold Spykman, TÜV Nord, Germany
15. Dry Storage Facility in Dukovany NPP, Jiri Gerza, Dominik Král, NPP Dukovany, Czech Republic
16. Experience and Challenges from 60 years of Dry Storage of Metallic Uranium Research Reactor Spent Fuel, Peter Bennett, Norwegian Nuclear Decommissioning (NND), Norway

17. Generic Cask Modelling Options to promote both Exchange and Comparability and their Illustration using a Muographic Application, Thomas Braunroth, Gesellschaft für Anlagen – und Reaktorsicherheit (GRS) gGmbH, Germany
18. Non-invasive Imaging of Transport and Storage Casks, Michael Wagner, Helmholtz Zentrum Dresden Rossendorf (HZDR), Germany
19. On the Applicability of the Master Curve Concept for Ductile Cast Iron based on Experimental and Microstructural Results, Marcel Holzwarth, Materials Testing Institute University Stuttgart (MPA), Germany
20. Adaptive Service Life Management for Concrete Building Structures of Interim Nuclear Storage Facilities, Stephan von Wehren, Technische Universität Braunschweig (TU-BS), Germany

2.1 Evaluation of Load Scenarios for Spent Fuel Assemblies

Kai Simbruner

Gesellschaft für Anlagen – und Reaktorsicherheit (GRS) gGmbH, Germany

The project investigates handling scenarios of spent nuclear fuel (SNF) assemblies, focusing on the additional loads imposed during cask drop scenarios from low heights (e.g. 30 cm) without impact limiters. Building on prior analytical and numerical strategies, the current study employs finite element analyses (FEA) in LS-Dyna to simulate these conditions, refine modeling approaches, and enhance expertise in structural response evaluation.

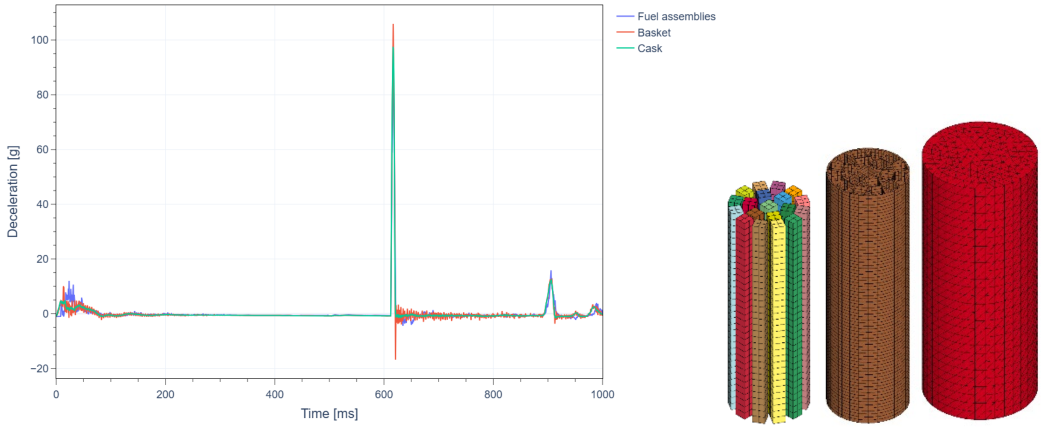

Fig. 1: Averaged deceleration time histories of fuel assemblies, basket, and cask subjected to a 60° cask drop

A simplified cask FEA model simulates low-energy drops, representing the cask as a single cylindrical body with homogenized elastic-plastic properties and an internal cavity, the basket as a linear-elastic simplified structure, and fuel assemblies as homogenized cuboids matching detailed dimensions. The ground uses a refined WINFRITH concrete model (MAT084). Drops initiate from the lowest point with 2.4 m/s velocity and gravity, across orientations like side (90 °), end (0 °), and slapdown angles. Time histories of displacements and decelerations (see Fig. 1) are computed for all components, with clearances minimizing initial gap influences; peak decelerations occur during secondary slapdown impacts. The results for cask, basket, and individual fuel assemblies highlight position-dependent responses, enabling extraction of basket cell kinematics as boundary conditions for SNF models.

Fuel rods employ beam elements with circular cross-sections and combined cladding-fuel properties (density, elasticity, bending stiffness). Guide tubes use tubular beams rigidly tied grids via spotweld constraints. Spacer grids evolved from four-node shells (two per side) to robust two-node beams (four per side, varying thickness by position), connected via nonlinear springs and dimples. The basket cell is rigid with prescribed motion from 30 cm drop video analysis and time histories derived from the cask drop model.

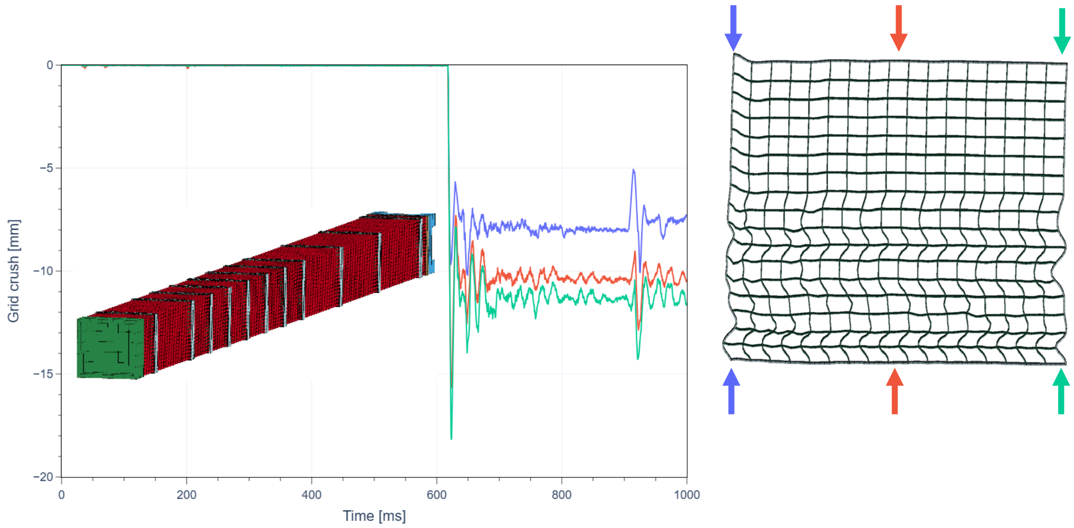

Fig. 2: Time history of spacer grid crush and deformed grid geometry for the fuel assembly model subjected to a 60 ° cask drop

Validation against surrogate assembly drop tests compares grid crush across positions with good agreement. As illustrated in Figure 2, for 60 ° cask drops, results reveal grid crushing and buckling as key energy dissipation mechanisms, thereby altering the rod pitch. The fuel rod deflection is governed by the grid and ultimately limited by the basket cell, resulting in rod-to-rod contacts.

The coupled framework of the cask model feeding SNF simulations enables comprehensive scenario analysis. A follow-up project from July 2025 will expand to detailed concrete models and seismic loads as accident conditions.

2.2 The Impact of Cooling Rate and Hydrogen Concentration on Hydride Morphology in Zircaloy-4

P. Kaufholz[1], *F. Boldt, T. Neikes, M. Stuke, A. M. Alvarez, M. Segerberg*

Gesellschaft für Zwischenlagerung mbH (BGZ), Germany

Hydride re-orientation may reduce ductility in zirconium-based cladding materials during extended dry storage. Therefore, investigations on hydrogen behavior are crucial to ensure safety of dry storage over extended time spans. This study investigates hydrogen behavior in un-irradiated Zircaloy-4 cladding tubes under conditions relevant to interim dry storage focusing on hydrogen precipitation, diffusion and hydride morphology. The effects of cooling rate and total hydrogen concentration on zirconium hydride morphology were investigated by exposing samples of certain hydrogen concentrations to varying cooling rates. Experiments were conducted, giving particular interest to hydride morphology under four distinct cooling rates across four hydrogen concentrations. In addition, a hydrogen diffusion experiment on an un-irradiated pre-hydrided tube segment exposed to a constant temperature gradient was performed to investigate on axial hydrogen re-distribution.

Results indicate a significant influence of cooling rate on zirconium hydride precipitation. The number of hydrides was found to increase with increasing cooling rate, while the size of hydrides decreases. Furthermore, an orientation effect was observed, showing randomly oriented hydrides for fast cooling, while slow cooling leads to long circumferential oriented hydrides. Figure 1 shows the development of zirconium hydride size and number with decreasing cooling rate for the 52 ppm samples as an example.

[1] Corresponding author: peter.kaufholz@bgz.de

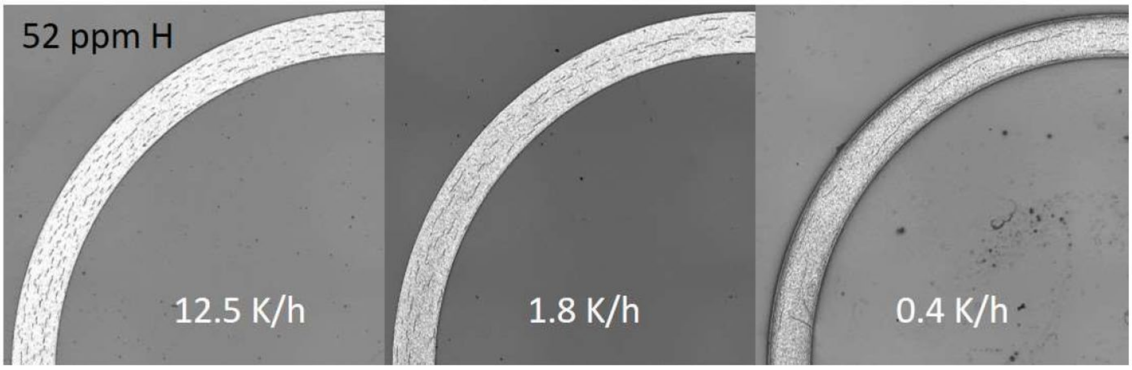

Fig. 1: Overview to hydride morphology of four different cooling rates across the sample matrix of 4 different hydrogen concentrations

An increase in hydrogen concentration leads to a higher number of hydrides, with a notable reduction in the impact of concentration at faster cooling rates. Samples with hydrogen concentrations above hydrogen solubility were assumed to contain non-dissolved hydrides at the maximum test temperature. For those samples the impact of cooling rate on hydrogen size and number was minimized, showing no variation in hydride size and number throughout different cooling rates. Figure 2 shows an overview to the effect of varying hydrogen concentrations on the morphology of zirconium hydrides at a constant cooling rate of 1.8 K/h.

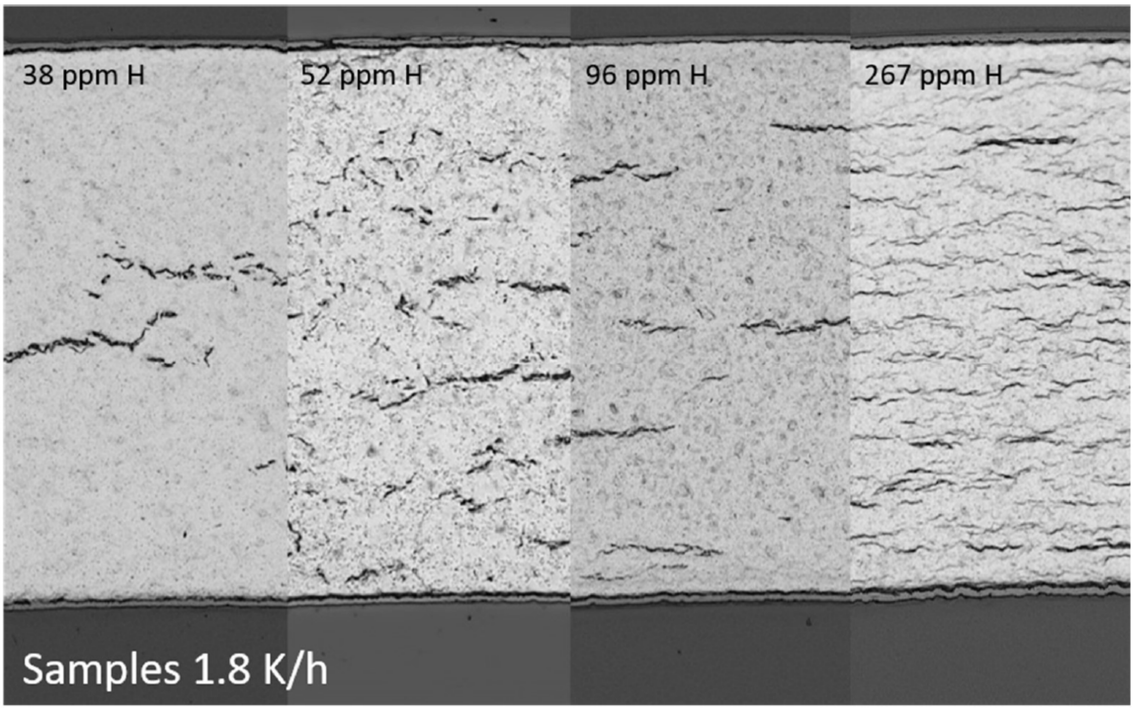

Fig. 2: Development of the zirconium hydride number at different hydrogen concentrations for a constant cooling rate of 1.8 K/h

The experiment on hydrogen diffusion along a constant temperature gradient showed a reversal in the hydrogen concentration gradient of the specimen. Also, the final hydrogen gradient as a result of thermo diffusion was found to be small and within the measurement uncertainties of the method. Figure 3 shows the results of the hydrogen diffusion experiment.

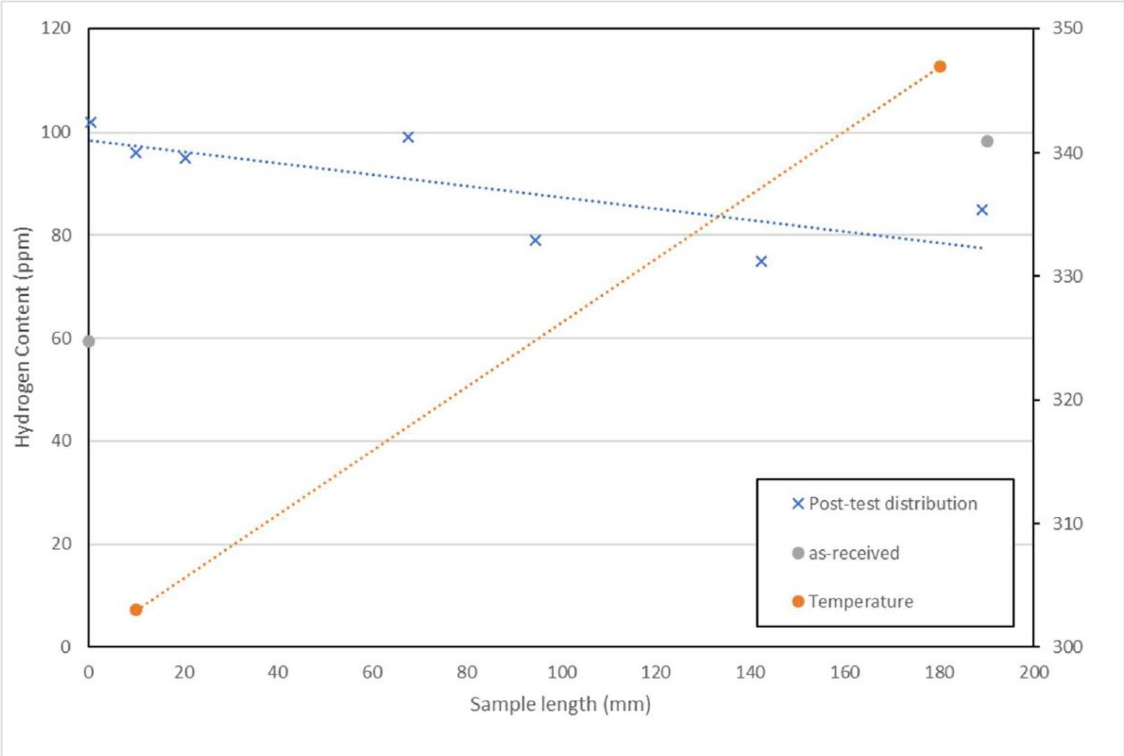

Fig. 3: Results of the hydrogen diffusion experiment along a thermal gradient showing initial hydrogen concentration at both Ends (gray circles), post test hydrogen measurements (blue crosses) and the temperature along the sample (orange circles)

These results underscore the importance of realistic boundary conditions for dry storage safety assessments. The findings also provide valuable input for experiments involving spent nuclear fuel such as BGZ's research project LEDA (Long-term Experimental Dry storage Analysis).

2.3 Mechanical Properties of Irradiated Zircaloy Cladding and Their Impact on Structural Integrity During Dry Interim Storage

Y. Lin[2], M. Vrellou, M. Herm, T. König, V. Metz, Ch. Kirchlechner

Karlsruhe Institute of Technology, Germany

The management of spent nuclear fuel (SNF) in Germany foresees direct disposal in a deep geological repository becoming available after 2050. In the interim, SNF assemblies are stored in dual-purpose casks (DPC) within dry storage facilities. As delays in repository commissioning are likely to exceed the licensed DPC storage periods, safe handling of SNF assemblies may require storage durations of up to 100 years [1], [2]. Understanding how the mechanical and chemical properties of Zircaloy-4 cladding evolve over time is essential for evaluating the safety of long-term dry storage.

This work investigates the microstructural and micromechanical behavior of non-irradiated Zircaloy-4 cladding-both hydrogenated and un-hydrogenated-as a means to develop and validate characterization methodologies for application to irradiated cladding extracted from medium and high burn-up uranium dioxide (UOX) and mixed oxide (MOX) fuel rods irradiated in commercial pressurized water reactors. Electron Backscatter Diffraction (EBSD), Vickers hardness testing, and nanoindentation were employed to characterize grain morphology, crystallographic texture, and localized mechanical properties. Particular emphasis was placed on optimizing surface preparation methods-including mechanical polishing, electropolishing, and Focused Ion Beam (FIB) polishing-to reconcile the differing surface quality requirements of these techniques. Hydride phase identification and apparent stability are highly sensitive to the chosen surface preparation method.

EBSD mapping revealed pronounced microstructural heterogeneity in the samples, with grain sizes ranging from ~0.2 μm to over 20 μm and high dislocation densities attributed to cold rolling and stress relief during manufacturing. Preliminary identification of hydride phases was achieved via EBSD on both mechanically polished and electropolished cladding samples, suggesting significant local variability in cladding microstructure. Vickers hardness testing and nanoindentation were conducted to obtain initial micromechanical data, including hardness and reduced modulus. Intensity maps revealed elevated values

[2] Corresponding author: *tzu.lin@kit.edu*

in hydride regions compared to the surrounding matrix and an overall increase in hardness for hydrogenated cladding relative to non-hydrogenated counterparts under identical testing conditions.

Future efforts will focus on refining electropolishing parameters, optimizing EBSD acquisition settings, and conducting selective nanoindentation to investigate local mechanical properties, particularly at the hydride-matrix interface. Thereafter, it is envisaged to apply the refined methodology to actual medium and high burn-up SNF cladding samples (UOX and MOX), previously being in contact with the fuel stack, as well as cladding specimens originating from the plenum section of a fuel rod.

References

[1] ESK-Positionspapier: Verlängerte Zwischenlagerung bestrahlter Brennelemente und sonstiger hochradioaktiver Abfälle in Abhängigkeit von der Auswahl des Endlagerstandorts, Nuclear Waste Management Commission (Entsorgungskommission), 23.03.2023.

[2] G. Spykman, Dry storage of spent nuclear fuel and high active waste in Germany – Current situation and technical aspects on inventories integrity for a prolonged storage time, Nuclear Engineering and Technology, 50, 313 - 317, 2018.

2.4 New Results in the Framework of the SPIZWURZ Project

Sarah Weick, Mirco Große, Mikhail Kolesnik, Conrado Roessger, Juri Stuckert, Martin Steinbrueck

Karlsruhe Institute of Technology, Germany

With delays in the commissioning of final nuclear waste repositories like in Germany, the interim dry storage of spent nuclear fuel (SNF) may extend several decades. Ensuring the structural integrity of cladding tubes over such prolonged storage periods requires a detailed understanding of its mechanical and microstructural evolution under interim dry storage conditions. Of particular concern is the migration and precipitation of hydrogen within zirconium-based alloys, eventually leading to hydride reorientation and embrittlement. However, existing data and predictive models are often based on short-duration laboratory experiments, extrapolated over long timeframes. To address this knowledge gap, the SPIZWURZ (Strain-Induced Hydrogen Redistribution in Fuel Cladding Tubes During Long-Term Interim Storage) project was initiated, focusing on realistic experimental conditions and code validation.

A central component of SPIZWURZ was the LICAS-01 bundle experiment, conducted at the Karlsruhe Institute of Technology. This large-scale test subjected a bundle of 21 fuel rod simulators, each 2.5 m in length and filled with ZrO_2 ring pellets and pressurized krypton gas, to a controlled thermal transient over 250 days. The bundle was constituted of three commercial zirconium-based cladding materials: Zircaloy-4, optimized ZIRLO™, and DX D4. Each alloy type was tested with two hydrogen concentrations (100 and 300 wt.ppm) and two internal pressures (106 and 146 bar), corresponding to hoop stresses of approximately 68 and 93 MPa. After reaching the peak temperature of 400 °C, the bundle was uniformly cooled to replicate the slow thermal decline of interim dry storage.

Post-test examinations, including both non-destructive and destructive methods, revealed distinct alloy-specific behavior with respect to creep deformation and hydride reorientation. Optimized ZIRLO™ exhibited the highest creep deformation with values up to four times higher than these of the other alloys. Nevertheless, it displayed remarkable resistance to hydride reorientation (see Fig. 1). In contrast, Zircaloy-4, particularly under high hoop stress and low hydrogen conditions, showed significant radial hydride formation. DX D4 exhibited an unique pattern of hydrogen accumulation in the liner, suggesting a complex redistribution behavior.

These observations were not predicted by modeling tools in a blind benchmark exercise conducted simultaneously to the experiment, underscoring the need for more robust experimental data to refine code predictions. Moreover, thermal-mechanical gradients within the bundle cross-section, such as elevated temperatures at the center, were found to influence local creep behavior, highlighting the multi-scale nature of the phenomena involved.

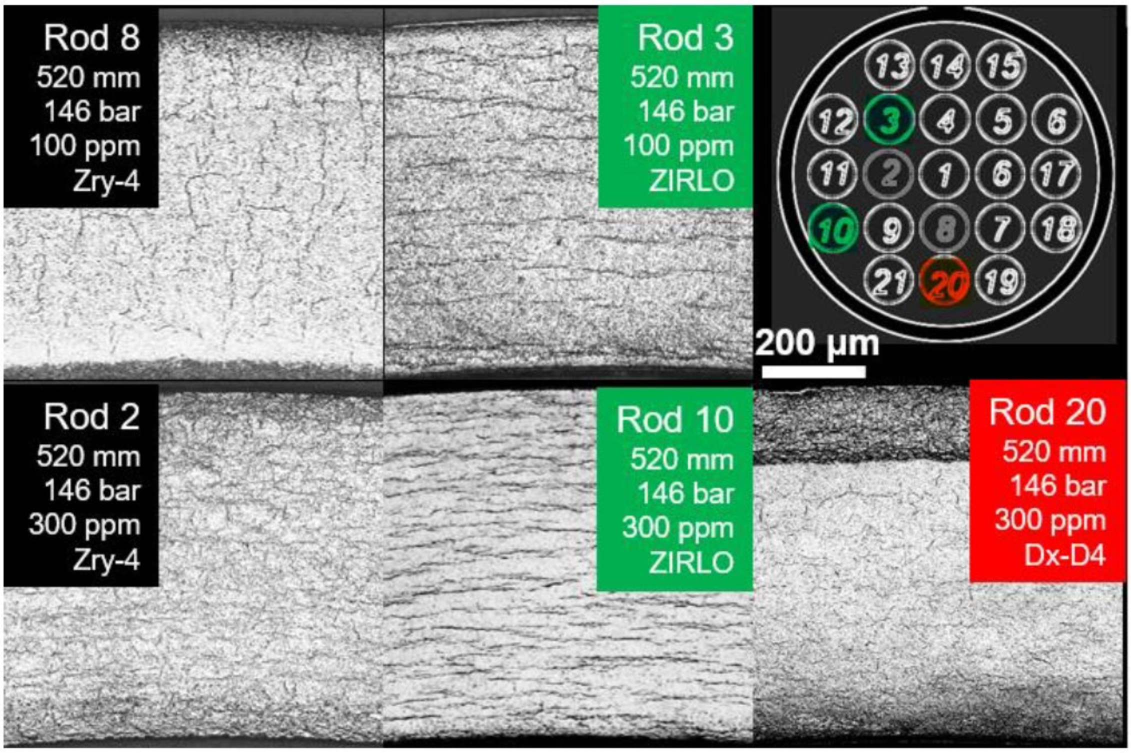

Fig. 1: Bundle cross section and optical micrographs of rods with the maximum inner rod pressure taken from the hottest zone (520 mm elevation), showing differences in the post-test hydride orientation

2.5 SPIZWURZ Blind Benchmark

Aleksandra Rezchikova

Gesellschaft für Anlagen – und Reaktorsicherheit (GRS) gGmbH, Germany

The assessment of fuel integrity during the entire dry storage period relies strongly on numerical simulations because an accurate reproduction of real dry storage conditions is impossible due to time constraints and safety issues associated with the use of irradiated materials. Therefore, the development of decent numerical tools is of great importance. These tools, however, have to be validated against the experiments at dry storage relevant conditions, such as the SPIZWURZ bundle experiment.

The SPIZWURZ benchmark was initiated within the frame of the SPIZWURZ project to validate and improve creep and hydrogen behavior modeling in the existing fuel performance codes. The benchmark is based on the SPIZWURZ bundle test performed at the LICAS facility of KIT, where a bundle of 21 electrically heated fuel rod simulators was slowly cooled over 250 days with a maximum averaged cooling rate of 0.94 °C/d. The experimental matrix included three materials (Zry-4, opt.ZIRLO, DX D4), two pressurization levels (103 and 142 bar), and two hydrogen concentrations (100 and 300 wppm). The initial bell-shaped temperature axial profile encompasses a wide range of temperatures, ranging from 405 to 86 °C, which includes different conditions that might arise during dry storage.

The currently running blind phase of the benchmark aims to investigate the ability of the existing codes to reproduce the creep and hydrogen behavior during the bundle experiment. Ten organizations from seven different counties contributed to the benchmark exercise. Since the metallographical probe analysis is still ongoing, only the benchmark creep results will be discussed.

The existing modeling approaches showed a good capability to predict Zry-4 and DX D4 creep strains, whereas the creep strains of opt.ZIRLO were underpredicted

2.6 Modelling Hydride Re-distribution and Re-orientation in DX Cladding

Martin Zemek

Axpo Power AG, Switzerland

The hydride morphology is a good indicator for assessment of ductility of the cladding and is therefore relevant for the spent fuel integrity during post-storage handling and transport operations [1 - 3]. Previously we have predicted a positive effect of the liner of bi-metallic cladding types to the hydride morphology up to the freedom of the base material from the hydrides during and after the storage [4]. Consequently, Axpo responded the invitation of GRS to blind benchmark of modelling the SPIZWURZ experiment [5] and transmitted the predictions of the creep strains and hydride morphologies for the Zry-4 and DX samples. In the workshop the comparison of the calculations with experiment and detailed model description are presented. For modelling hydrogen re-distribution and hydride formation the HyReL code was used. Here the rods were represented by a 2D cylindrical geometry resolved axially by 14 nodes and radially by 5 ring sections, the outermost section representing the outer liner. For the blind benchmark, initially a homogeneous initial radial hydrogen distribution across the cladding wall was conservatively assumed. Later, the calculations were repeated with the realistic initial condition of the DX tubes. The comparison of calculations with the post-test metallography of the rod 20 is shown in Figure 1. The model predictions fit qualitatively the currently available metallography while the post-test amount of hydrogen in the base material of DX cladding is very limited compared to the monometallic Zry-4 tubes.

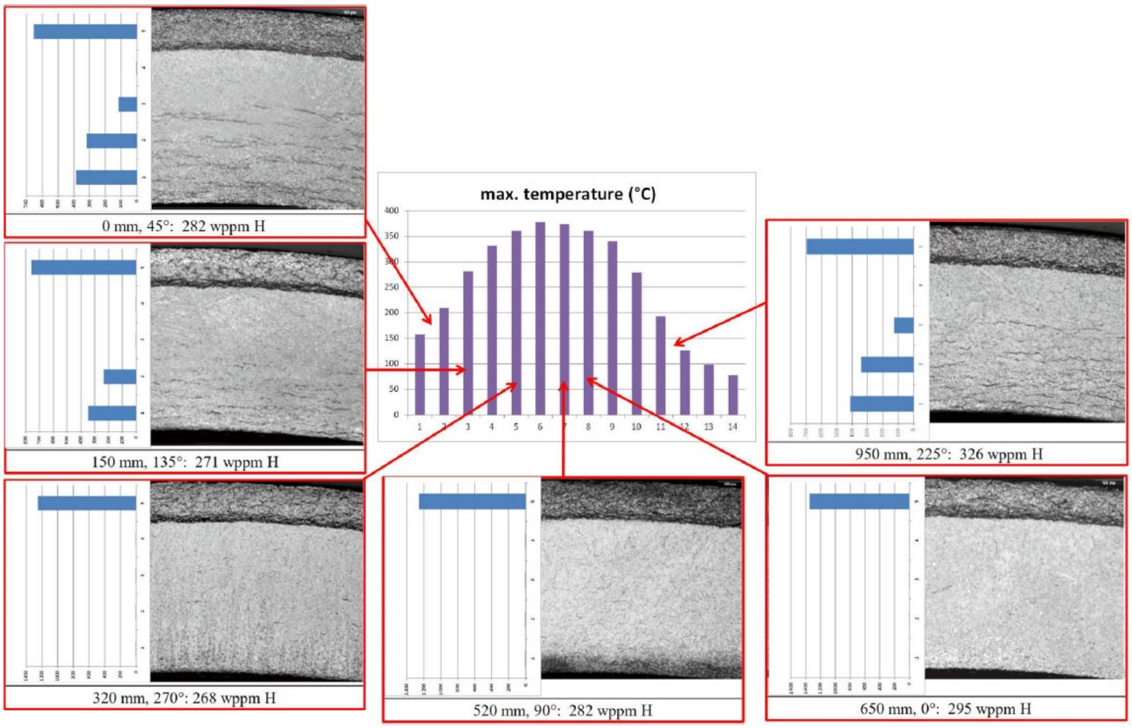

Fig. 1: Qualitative comparison of the calculations with the metallography micro-photographs of the rod 20 at different sections

The temperature scale indicates the maximum temperature of the individual nodes at the beginning of the test [6]

The HyReL code consists of three main components: 2D diffusion model (Fick's law), phase change model and a hydride re-orientation model. The diffusion equation is enhanced by a term describing the hydrogen potential gradient according to the concept by [7]. Several material correlations are available in the code, and for simulation of the SPIZWURZ experiment, the correlations were selected that showed a very good performance during validation runs: diffusion coefficient according to [8] corrected by the volumetric fraction of α-phase; thermo-diffusion coefficient and the hydride precipitation model (HNGD) according to [9]; hydride dissolution correlation derived from [10] corrected by the α-phase fraction; solid solubilities for Zry-4 according to [11] for TSSd and according to [12] for TSSp and custom description of TSSd and TSSp for D4 alloy in DX/D4 [4] with the hydrogen potential difference of $\Delta\mu_0$ = -567 J/mol. The correlation for the radial hydride formation according to EPRI [13] was enhanced by a structural factor considering the hydrides already present in the cladding wall:

$$F_R = \frac{F_\sigma}{a \cdot (c_{PP} - c_R + b)^2} \qquad \begin{aligned} a &= 6.25 \cdot 10^{-6} \\ b &= 400 = 1/\sqrt{a} \end{aligned}$$

Where F_R is the fraction of hydrides precipitating in radial direction, Fσ is the reorientation factor by [13], c_{PP} the concentration of hydrides present (ppm), c_R the amount of radial hydrides (ppm) and a (ppm^{-2}) and b (ppm) are constants. The reorientation correlation itself is sensitive to precipitation kinetics reflecting the results of studies with differing cooling rates.

The model results were analyzed and further simulations were performed to evaluate an in-cask behavior without fast temperature fluctuations. It was shown, that the effect of the stepwise cool-down and of temperature fluctuations during the SPIZWURZ experiments promote the hydrogen migration towards the liner of DX cladding (see Fig. 2) but they promote also formation of radial hydrides. However, the final post-test state of the cladding was very similar for both temperature histories but extension of the hydride-free zone. Generally, the presence of liner provides a reduction of the hydride concentration in the base material of DX cladding up to a practical hydride-freedom during the cool-down and restraints the formation of radial hydrides in areas the initial temperature is too low to achieve such a hydride-free state.

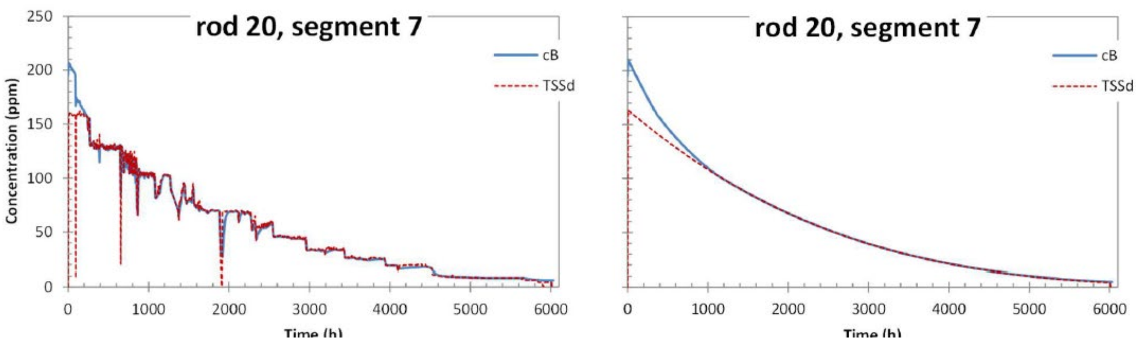

Fig. 2: Comparison of the code predictions of the overall hydrogen concentration in the base material c_B during the experiment (left) and during a smooth linear cool-down (right)

Final comment:

The hydride morphology is a good one, but still an indicator only, therefore direct ductility measurements (RTT or RCT) are highly recommended. Furthermore, the ductility of Zry tubing is an anisotropic property. Real conditions and loads have to be considered while drawing conclusions for safety of transportation and handling of spent fuel.

References

[1] Bouffioux P. et al., TopFuel2013, Charlotte, NC (USA), September 15-19, 2013 «Hydride Reorientation in M5 Cladding and Its Impact on Mechanical Properties».

[2] Kook D., Proceedings of the 17th Inter-national Symposium on the Packaging and Transportation of Radioactive Materials PATRAM2013, San Francisco, CA (USA), August 18-23, 2013 «Hydride Re-Orientation Test for Spent Fuel Integrity».

[3] Daum R. et al., Journal of Nuclear Science and Technology, Bd. 43, Nr. 9, pp. 1054-1067, 2006 «Radial-hydride Embrittlement of High-burnup Zircaloy-4 Fuel Cladding».

[4] Zemek M. et al., ENS TopFuel conference held on October 24-28 2021 in Santander (E), paper 079, «Effects of the Liner on the Ductility of Claddings after the dry Storage».

[5] Rezchikova A. et al., Proceedings of the 8th Workshop on the Safety of the Extended Dry Storage of Spent Nuclear Fuel, GRS, 15-17th May 2024, «SPIZWURZ Benchmark for simulation of hydrogen behaviour in fuel rod claddings at dry storage relevant conditions. Phase 1 (Blind tests)».

[6] metallography by courtesy of Gesellschaft für Anlagen- und Reaktorsicherheit (GRS) gGmbH and Karlsruhe Institute of Technology.

[7] Gong W. et al., Journal of Nuclear Materials, 526, 151757, 2019 «Hydrogen diffusion and precipitation in duplex zirconium nuclear fuel cladding quantified by highresolution neutron imaging».

[8] Zhang Y. et al., Nature Scientific Reports 7, 41033, 2017 «Anisotropic hydrogen diffusion in α-Zr and Zircaloy predicted by accelerated kinetic Monte Carlo simulations».

[9] Lacroix E., Dissertation at the Pennsylvania State University, 2019 «Modelling Zirconium Hydride Precipitation and Dissolution in Zirconium Alloys».

[10] Kammenzind B.F. et al., Zirconium in the Nuclear Industry: Eleventh International Symposium, ASTM STP 824 (1984), pp. 338-370 «Hydrogen Pickup and Redistribution in Alpha Annealed Zircaloy-4».

[11] Kearns J.J., Journal of Nuclear Materials 22 (1967) 292-303 «Terminal Solubility and Partitioning of Hydrogen in the Alpha Phase of Zirconium, Zircaloy-2 and Zircaloy-4».

[12] Torres É. et al., Fontevraud 8: Conference on Contribution of Materials Investigations and Operating Experience to LWRs' Safety, Performance and Reliability, Avignon (F), 15-18 Sep 2014 «Adsorption and Diffusion of Hydrogen in Zircaloy-4».

[13] Liu W. et al., Top Fuel 2016, Boise, ID (USA), September 11-15, 2016 «A Hydride Reorientation Model for Irradiated Zirconium Alloy Cladding».

2.7 CIEMAT´s HYDCLAD Tool - Contribution to SPIZWURZ Benchmark

F. Feria, C. Aguado, L.E. Herranz

Unit of Nuclear Safety Research, CIEMAT, Spain

Fuel safety research in dry interim storage addresses those mechanisms that may jeopardize the cladding integrity of the spent fuel. Dry storage conditions may foster cladding degrading mechanisms such as creep (viscoplastic deformation) and hydrides radial reorientation. The latter involves distribution, precipitation and reorientation of the hydrogen picked up during irradiation and it might significantly reduce the material resistance to failure. In this context, it is of utmost interest to have reliable analytical capabilities to predict the cladding performance under the prevailing conditions. Modelling of hydrogen behaviour is fundamental to accurately characterize cladding mechanical state, particularly important if transient mechanical loads come into play (e.g. handling/transport accidents).

CIEMAT developed a model describing in-clad hydrogen performance, HYDCLAD. It encompasses diffusion and thermo-diffusion as drivers of the atomic hydrogen migration, precipitation of zirconium hydrides as a sink of the cited migration, and hydrides radial reorientation under dry storage. The development and assessment details of the modelling carried out is shown elsewhere (Feria and Herranz, 2018; Feria et al., 2020; Feria and Herranz, 2023).

The latest activities with HYDCLAD have dealt with the implementation and validation of an alternative hydrogen precipitation model, the so-called Hydride Nucleation-Growth-Dissolution (HNGD) model (Passelaigue et al., 2022). The former option is based on the classic modelling where there is hysteresis in the solubility limit (i.e., precipitation and dissolution limits) and the precipitation kinetics are independent of the hydrides formed. The HNGD model is a more phenomenological approach that accounts for nucleation and growth of the hydrides. The assessment of this HYDCLAD extension has been carried out under representative in-reactor conditions, which has allowed concluding that a re-parameterization of the HNGD model enhances the classic approach in terms of hydrides rim prediction (Feria and Herranz, 2023).

The present work provides further assessment of HYDCLAD under dry storage conditions. It has been done against a database from Desquines et al. (2014) (tests on unirradiated cladding), and through CIEMAT’s contribution to the SPIZWURZ benchmark (Rezchikova and Stuckert, 2024), where experimental data are becoming available for validation. Since cladding creep is also considered in the cited benchmark, a creep law derived by CIEMAT for FRAPCON-xt (extension to dry storage of the FRAPCON fuel performance code) (Feria and Herranz, 2011; Feria et al., 2015) has also been evaluated. It should be noted that according to the validity of the CIEMAT's models, the contribution to the SPIZWURZ benchmark has been focused on Zry-4 rods.

Concerning the assessment against the database from Desquines et al. (2014), Figure 1 shows the model-to-data comparison in terms of the radial hydrides content. The graphs depict the HYDCLAD evaluation both with and without the modelling extension. In the case of simulations with the classic precipitation approach, there is a trend to increasingly underestimate hydrides content as the experimental values rise, although the modelling uncertainties capture the error in approximately 90 % of the cases. Regarding the simulations with the HNGD model, the trend to underestimate disappears, particularly above 150 wppm, and there are still acceptable predictions taking into account the uncertainties (error captured in about 85 % of the cases). In both cases the average relative error of the best estimate is around 28 %.

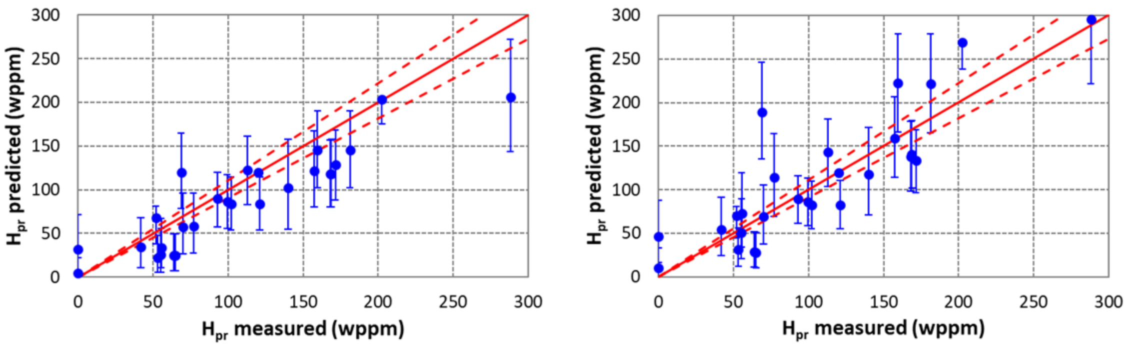

Fig. 1: Comparison of HYDCLAD predictions of radial hydrides, H_{pr}, against the database from Desquines et al. (2014)

Simulations with precipitation models: classic (left) and HNGD (right). Blue lines represent modelling uncertainty and red dotted lines data error

Regarding the evaluation carried out through CIEMAT´s contribution to the SPIZWURZ benchmark, Figure 2 shows, as an example, the comparison of the simulations with HYDCLAD activating the different precipitation models. It is expressed in terms of the radial hydrides content evolution in the rod 11 of the corresponding experiment. Note that the experimental data have not been released at the moment of this contribution. It should be highlighted that the classic precipitation modelling related results do not follow the thermal fluctuations observed in the experiment (see Rezchikova and Stuckert (2024)), while the HNGD model is capable of capturing these variations, giving rise to higher radial hydrides (in line with the results shown in Fig. 1). This is consistent according to the precipitation kinetics of each model, that is around hours in the classic approach and minutes in the HNGD model. Anyhow, sounder conclusions are expected when experimental data become available.

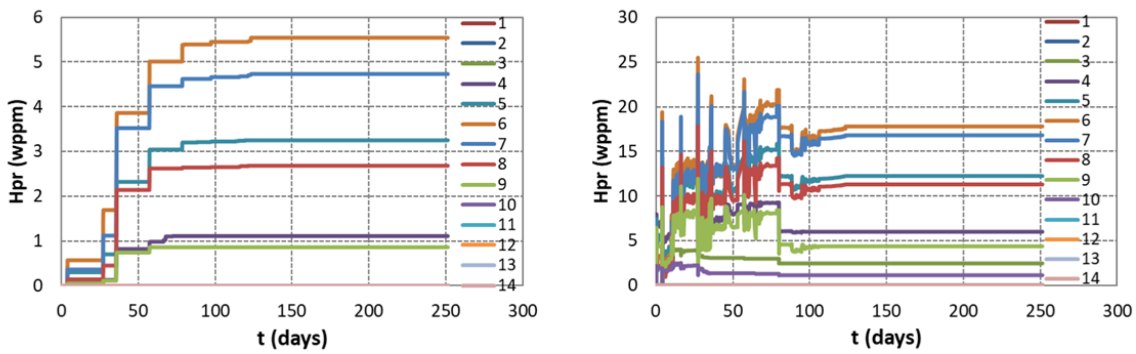

Fig. 2: HYDCLAD prediction of radial hydrides, H_{pr}, evolution under SPIZWURZ experiment conditions (rod 11) for each rod axial node (node 1 for bottom and 14 for top part)

Simulations with precipitation models: classic (left) and HNGD (right)

Finally, the evaluation of CIEMAT's creep law against data from the SPIZWURZ benchmark has given rise to consistent predictions from a qualitative point of view and acceptable accuracy (maximum relative errors below 20 %). As an example, Figure 3 depicts the model-to-data comparison in terms of creep axial profile of rods 2 and 4 at the end of the SPIZWURZ experiment. These cases show a good accuracy of the CIEMAT's law.

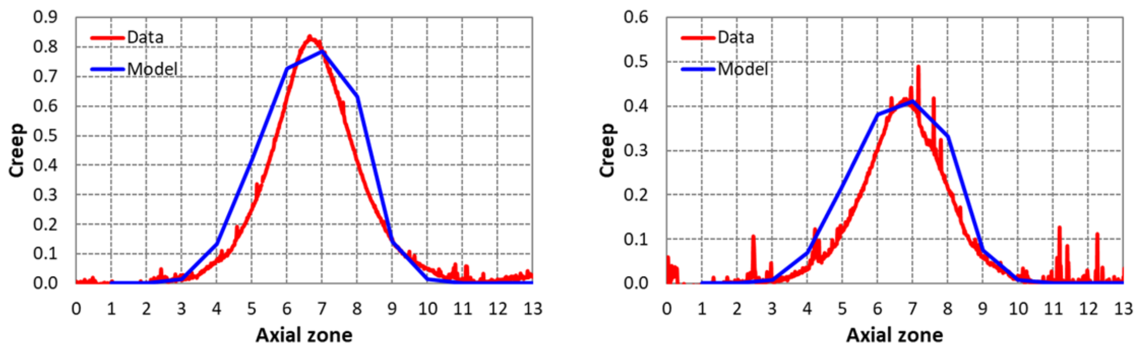

Fig. 3: Comparison of CIEMAT´s creep law predictions against data from SPIZWURZ experiment (rod 2 on the left and 4 on the right)

Acknowledgment

The authors wish to thank the Spanish Nuclear Safety Council for the funding of the work within the MATMEC project.

References

[1] Desquines, J., Drouan, D., Billone, M., Puls, M.P., March, P., Fourgeaud, S., Getrey, C., Elbaz, V., Philippe, M., 2014. Influence of temperature and hydrogen content on stress-induced radial hydride precipitation in Zircaloy-4 cladding. Journal of Nuclear Materials, 453, 131–150.

[2] Feria, F., Herranz, L.E., 2011. Creep assessment of Zry-4 cladded high burnup fuel under dry storage. Progress in Nuclear Energy 53, 395–400.

[3] Feria, F., Herranz, L.E., Penalva, J., 2015. On the way to enabling FRAPCON-3 to model spent fuel under dry storage conditions: The thermal evolution. Annals of Nuclear Energy, 85, 995–1002.

[4] Feria, F., Herranz, L.E., 2018. Effect of the oxidation front penetration on in-clad hydrogen migration. Journal of Nuclear Materials, 500, 349-360.

[5] Feria, F., Aguado, C., Herranz, L.E., 2020. Extension of FRAPCON-xt to hydride radial reorientation in dry storage. Annals of Nuclear Energy, 145, 107559.

[6] Feria, F., Herranz, L.E., 2023. Assessment of hydride precipitation modelling across fuel cladding: Hydriding in non-defective and defective fuel rods. Annals of Nuclear Energy, 188, 109810.

[7] Passelaigue, F., Simon, P-C.A, Motta, A.T., 2022. Predicting the hydride rim by improving the solubility limits in the Hydride Nucleation-Growth-Dissolution (HNGD) model. Journal of Nuclear Materials, 558, 153363.

[8] Rezchikova, A., Stuckert, J., 2024. SPIZWURZ Benchmark Phase 1. GRS report.

2.8 Framatome's Performance in SPIZWURZ Creep Benchmark

Radan Sedlácek, *Dietmar Deuble*
Framatome GmbH, Germany

Framatome GmbH participated in the SPIZWURZ creep benchmark [1] with the code CSAS that is normally used for dry storage Fuel Rod Design (FRD) calculations. The computer code CSAS conservatively calculates the dry storage design relevant quantities, namely the maximum cladding stress and maximum cladding creep strain, under given axial temperature profile as a function of time. The input to CSAS is the end-of-life (EOL) state of the fuel rod as calculated by the FRD code CARO-E: amount of gas, rod dimensions, rod free volumes, oxide thickness, and fast fluence. The program calculates the cladding tangential creep strain during storage conservatively by choosing an unfavorable combination of conditions (temperature, fluence, oxide thickness). For the benchmark calculations, a more flexible R&D version of CSAS was used, cf. [2]. It calculates the creep strain in several axial zones and is capable of dealing with the specific benchmark conditions, i.e. the mutually independent pressure and temperature input [1]. The cladding creep model used in CSAS (both FRD and R&D versions) is described in paper [3]. The model is implemented in CSAS with proprietary parameter values that were calibrated and validated on Framatome own cladding materials:

- Zry-4 and Duplex (several variants)
- Zry-2 RX
- $M5_{Framatome}$[3]

The calibration and validation database consists of about one hundred creep tests per material (irradiated and non-irradiated). The calibration was performed with practical FRD application in mind: possibly best-estimate, if not possible then conservative. Underestimation is allowed only for strain values negligible compared to the dry storage creep strain criterion of 1 % tangential strain.

[3] $M5_{Framatome}$ is a trademark or registered trademark of Framatome or its affiliates, in the USA or other countries.

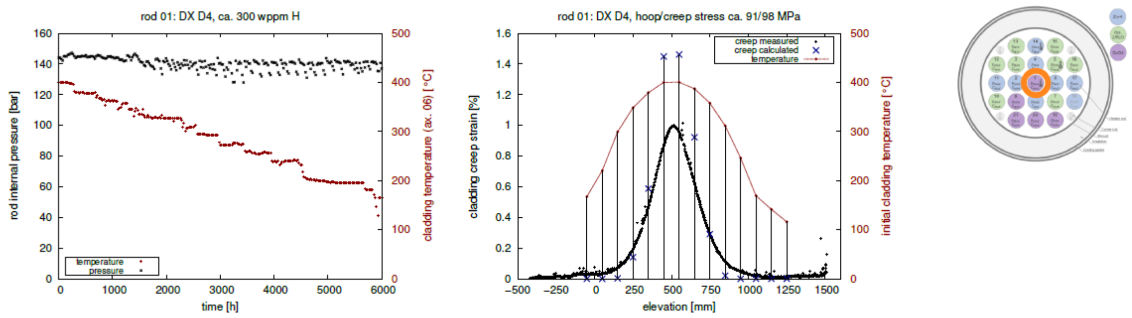

Fig. 1: The central rod

This pragmatic approach is reflected by the Framatome's SPIZWURZ creep benchmark results. Figure 1 shows the simulation of the central rod. Medium strains that are relevant for FRD are well reproduced, large strains are overestimated, small strains underestimated.

The Figures 2 and 3 show the effects of stress (98 versus 71 MPa) and temperature (inner versus outer ring) on creep strains. Both effects are well reproduced in the simulation results.

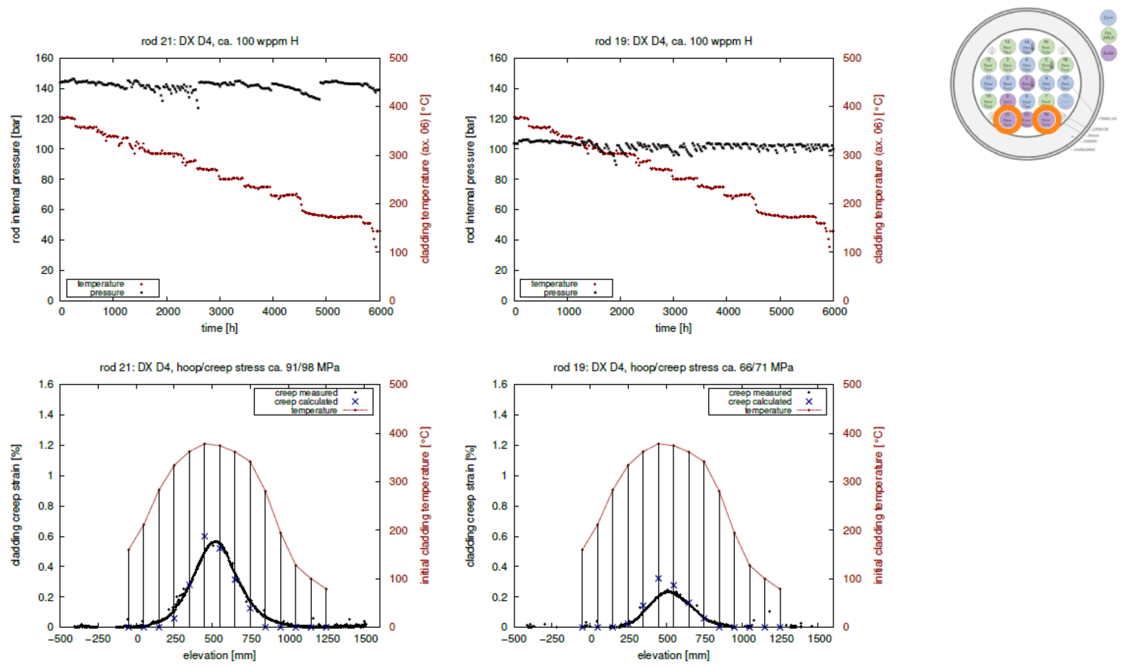

Fig. 2: Effect of stress on creep strain

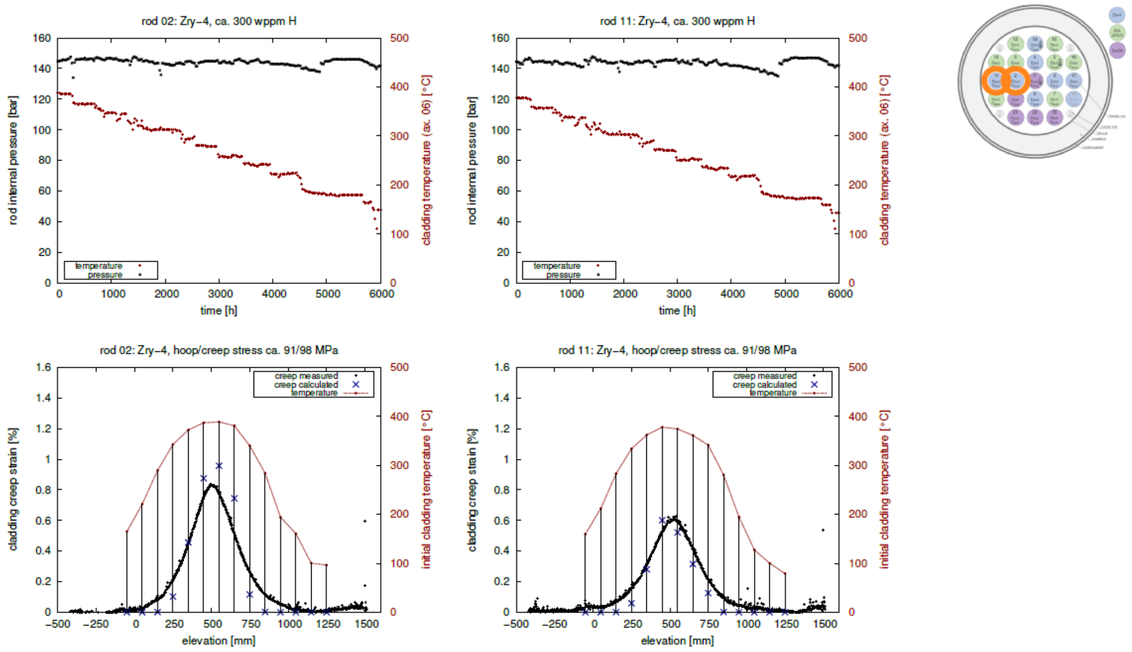

Fig. 3: Effect of temperature on creep strain

The Figures 4 and 5 show the effects of Hydrogen content (300 versus 100 ppm H) and cladding type (Zry-4 versus DX D4) on creep strains. Both effects appear to be negligible. They are not explicitly considered in the Framatome creep model.

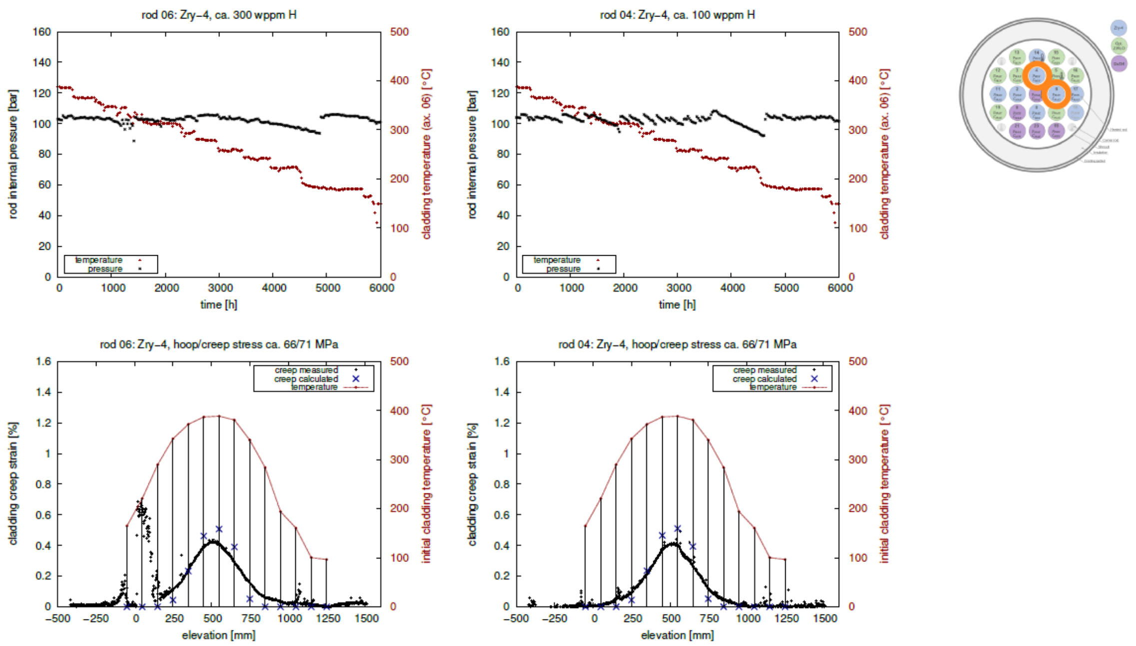

Fig. 4: Effect of Hydrogen on creep strain

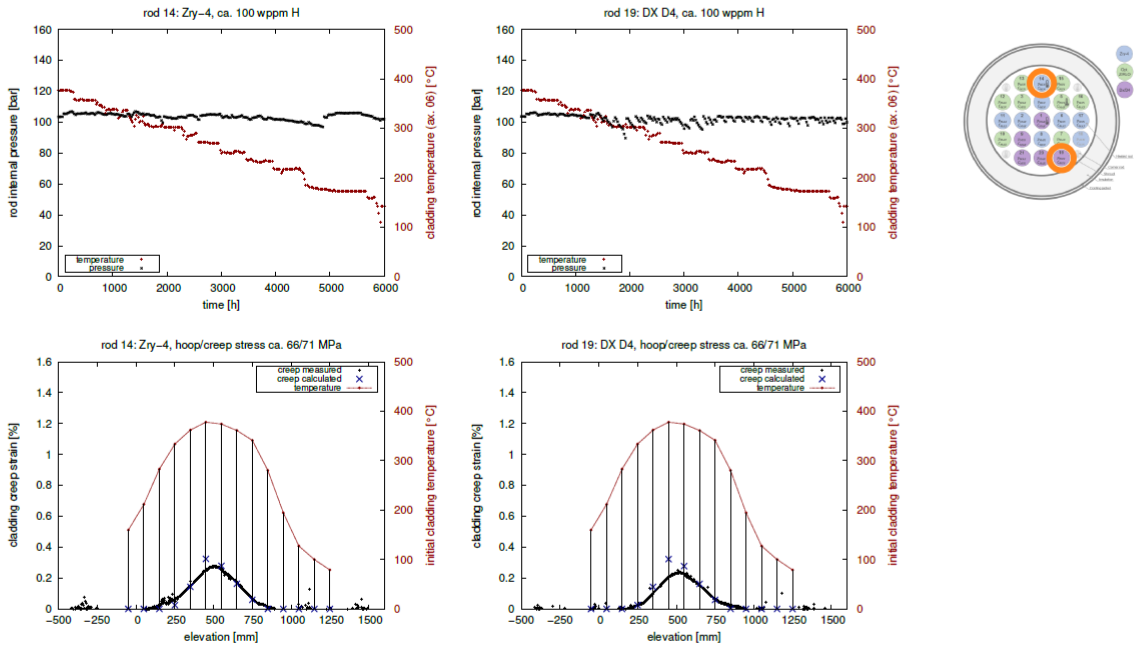

Fig. 5: Effect of cladding material on creep strain

The results of the SPIZWURZ benchmark confirm the calibration and validation of the Framatome cladding creep model for dry storage. The effects of stress and temperature on creep strain are well reproduced. The effects of Hydrogen content as well as the difference between Zry-4 und DX D4 are negligible and not considered by the Framatome creep model.

References

[1] A. Rezchikova and J. Stuckert. SPIZWURZ Benchmark Phase 1 Specification V.3. Technical report, GRS, July 2024.

[2] R. Sedlácek, D. Deuble, H. Landskron, and E. Schweitzer. Benchmark for thermo-mechanical fuel rod behaviour during dry storage. In F. Boldt, M. Stuke, and M. Péridis, editors, Benchmark on Thermomechanical Fuel Rod Behaviour, Phase I Report, pages 101{103. Gesellschaft für Anlagen- und Reaktorsicherheit (GRS) gGmbH, 2022. (4th GRS Workshop on Safety of Extended Dry Storage of Used Nuclear Fuel, e-Workshop, 3-4 June 2020, ISBN: 978-3-949088-62-9).

[3] C. Cappelaere, R. Limon, C. Duguay, G. Pinte, M. Le Breton, P. Bouffioux, V. Chabretou, and A. Miquet. Thermal creep model for CWSR Zircaloy-4 cladding taking into account the annealing of the irradiation hardening. Nuclear Technology, 177(2):257{272, 2012.

2.9 Numerical Investigations on Gd-Burnout of Fuel Assemblies with Low Burnup

V. Hannstein[4], *M. Stuke*

Gesellschaft für Zwischenlagerung mbH (BGZ), Germany

Modern boiling water reactor (BWR) fuel assembly designs regularly feature fuel rods containing Gadolinium as a burnable absorber. In these the reactivity of the fuel at low burnups is reduced by taking advantage of the large neutron capture cross-sections of Gd-155 and Gd157. The burnout of these nuclides early phase of fuel irradiation leads to increasing reactivity until a peak is reached at around 10 - 15 GWd/tHM after which it decreases monotonously till the end of irradiation.

In an ongoing international project called LAGER (Laser Ablation of Gadolinium Evolution Radially) [1] led by Studsvik together with Vattenfall a Gadonlinia-bearing fuel rod from a BWR fuel assembly with a burnup close to peak reactivity from a Swedish reactor was taken to the Studsvik hot labs in order to be analyzed. The main purpose is to gather nuclide concentration data from this fuel rod and providing data for the verification of computer models for the determination of nuclide concentrations in general and specifically the behaviour of the Gd-Isotopes. The interest of BGZ in this project comes mainly from the fact that there are low burnup BWR fuel assemblies in storage in Germany. The LAGER project offers a unique possibility to obtain data for code validation. Besides standard bulk dissolution mass spectroscopy measurements also measurement by Laser Ablation Inductively Coupled Plasma Mass Spectroscopy (LA-ICP-MS) are part of the project. These allow for measurements of the nuclide concentrations with high spatial resolution. By cutting out small samples from the rod 2D concentration maps across a cross-section of the fuel be obtained.

The present work shows first results of detailed 2D simulations that have been performed at BGZ in order to investigate the quality with which the burnout of Gadolinium can be captured by simulation and to compare nuclide concentrations predictions with measurements. The simulations were performed with the Monte Carlo neutron transport code Serpent [2] developed by VTT, Finland (version 2.2.1). Detailed geometrical models of the fuel assembly cross section were implemented with the sample rod being subdivided

[4] Corresponding author: volker.hannstein@bgz.de

into 10 radial and 12 azimuthal zones. In order to being able to compare the experimental data, which is given as a large set of point wise measurements, with the computational results given as zone averaged data, a number of post processing steps were done on the experimental data. These included data smoothing and an averaging over the individual fuel zones given by the simulation grid. The comparison was done by looking at the quotients C/E or at the values C/E-1 were C represents the value obtained from computation and E represents the experimental result. Overall four samples were analysed, one from the bottom part of the rod close to the lower blanket two from the upper end of the active zone and one sample taken from the central part of assembly.

Several different data representations were used to analyse the result including 2D color plots, bar plots of the showing the median and the spread of C/E values of a given nuclide across the simulated fuel pin segments, and plots of the C/E-values along cuts across the fuel pin in different axial direction. Overall, a good agreement between measurement and simulation was observed for many important nuclides. However, the simulations show a rather strong overprediction of the concentrations of Gd-155 and Gd-157 for the analysed samples. An example of this can be seen in Figure 1 which shows the variation of the C/E-1 values of a selection of measured nuclides for sample LA3 in the form of a box plot. There are several possible explanations for the overestimation of the Gd concentrations. Most importantly, the concentrations are very sensitive to a variation of the void fraction of the moderator, a quantity which may have a rather high uncertainty. 3D effects may also be of some importance. This includes an influence of the adjacent fuel assemblies as well as axial variations of the neutron flux. Finally, part of the observed deviations may arise from the small absolute concentrations of the relevant nuclides. It is planned to further investigate these aspects in more detail. In this context, the results from the bulk dissolution measurements will be of great value as soon as they become available, since they will provide an independent cross check of the experimental results obtained so far.

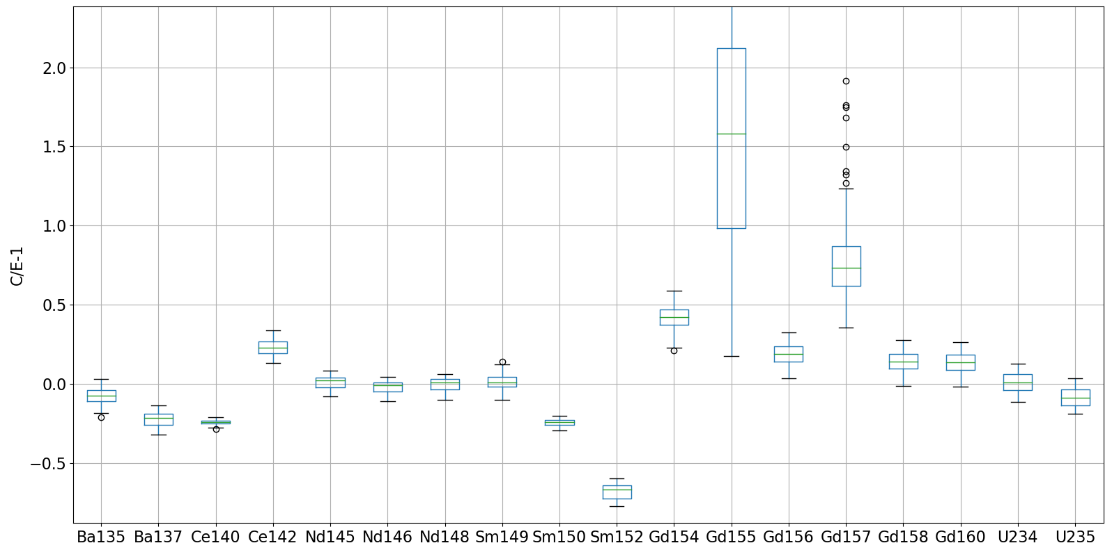

Fig. 1: Comparison of computed (C) to experimental (E) concentrations for a selection of nuclides for Laser Ablation ICP-MS sample LA3 in the form of relative deviations C/E-1

The Boxes represent the first and third quartile (Q1 and Q3) of the distribution of measurement data points for each nuclide. The whiskers represent the last data points extending no more than 1.5*IQR (IQR = Q3 − Q1) from the edges of the box. The dots are data values outside the borders represented by the whiskers

References

[1] P. Zsabka et al. “The Lager Project: Laser Ablation - ICP-MS Studies on Low burnup Gadolinia Doped UO2 Fuel - Supporting burnup Calculations With Spatial Resolution On The Micrometer Scale,” TopFuel 2024, Grenoble, 29 September – 3 October (2024).

[2] Leppanen, J., et al. “The Serpent Monte Carlo code: Status, development and applications in 2013,” Ann. Nucl. Energy, 82 pp. 142-150 (2015).

2.10 Calculation of Activation Products of the Structural Components of a Light Water Reactor (LWR) Spent Fuel Assembly using FISPACT-II

Rahul Narang

Technical University of Munich (TUM), Germany

N/A

2.11 Research at PSI in Respect to Intermediate Dry Storage - Current Work and Outlook

Johannes Bertsch

Paul Scherrer Institut (PSI), Schweiz

N/A

2.12 Fuel Performance Modelling of Used Nuclear Fuel Transfer between Storage Pools

P. Konarski, C. Cozzo, G. Khvostov, H. Ferroukhi
Paul Scherrer Institut (PSI), Schweiz

According to the Swiss nuclear fuel management policy, used nuclear fuel is planned to be disposed in a deep underground repository. Prior to final disposal, used nuclear fuel is stored at reactor sites and in a centralized dry storage facility. Since the operation dates of the final repository are unknown, extended periods of interim storage must be considered. A research program to investigate the fuel rod integrity during long-term dry storage has been launched at Paul Scherrer Institute. In the context of the project, fuel rod performance simulations are carried out with the code Falcon.

There are two used fuel pools at the Swiss nuclear power plant Gösgen, one inside and one outside the reactor building. The transfer of fuel in dry casks between them is known as the Wet-To-Dry-To-Wet (W2D2W) transport procedure. The process is associated with vacuum drying, transfer to an external storage pool and reflooding. The high cladding temperature and stress during the drying and transport in combination with quick reflooding can lead to precipitation of radial hydrides and deterioration of the cladding's mechanical properties. In this work, the impact of the drying, transfer and reflooding periods on the concentration of radial hydrides is studied. Multiple realistic scenarios considering various durations of the W2D2W stages are studied. The tested drying durations are 12 and 24 h. The transfer times are from 1 to 5 h. The reflooding durations are from 1 to 5 h as well.

Three fuel rods with different burnups, hydrogen concentrations, and Rod Internal Pressures (RIP) are selected for the analysis. They are referred to as the Highest RIP, Average RIP, and Lowest RIP rods.

The results show the impact of different phases and revealed that the reflooding has the biggest impact on the hydrogen behavior. The analysis of the simulated dry storage scenarios shows that the maximum temperature obtained at the end of drying governs the hydrogen migration into the liner of the DXD4 duplex cladding. Moreover, shorter reflooding leads to more hydrogen in the substrate as shown in Figure 1.

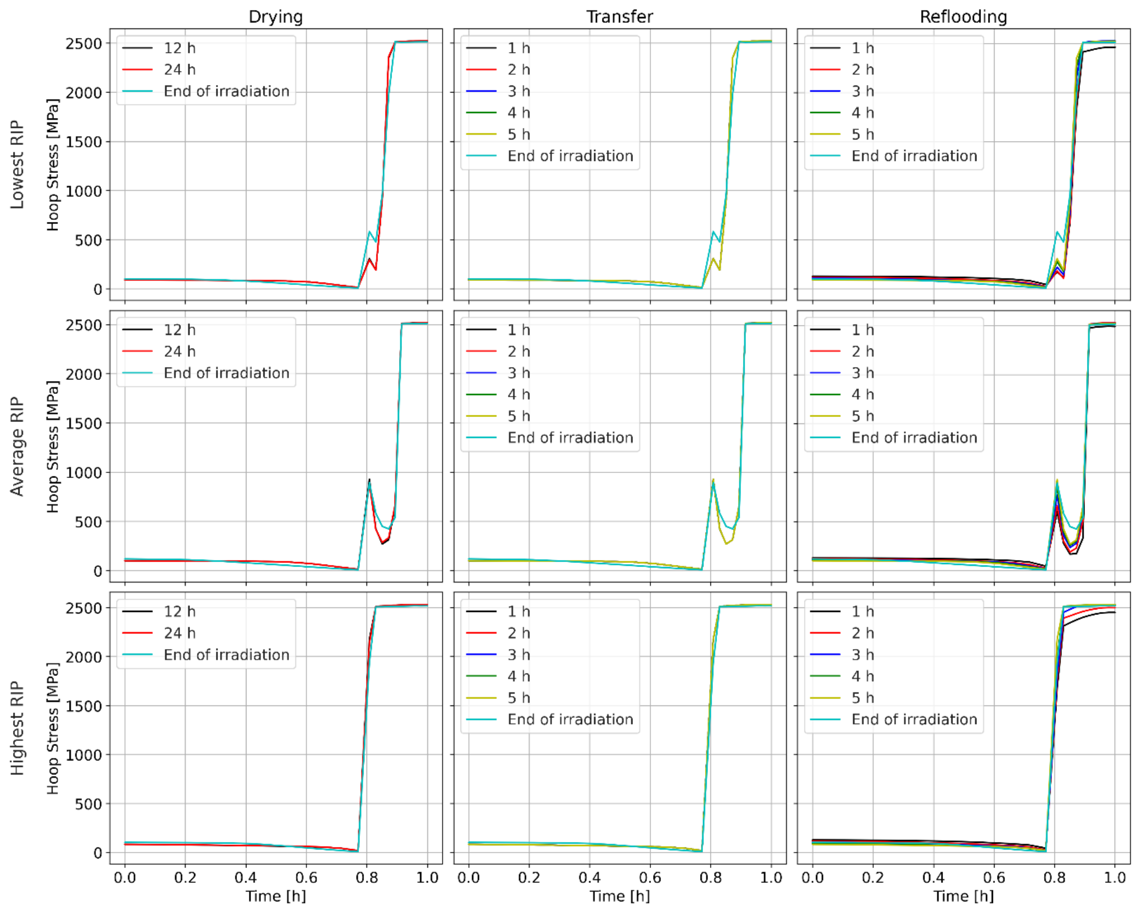

Fig. 1: Impact of different W2D2W phases on the hydrogen radial profiles calculated at the relative elevation of 0.5

Left column: impact of drying; middle column: impact of transfer; right column: impact of reflooding. Top row: Lowest RIP; middle row: Average RIP; bottom row: Highest RIP.

The W2D2W simulations are followed by dry storage scenarios with three different maximum cladding temperatures: 200 °C, 250 °C and 300 °C. The simulations showed that the cladding stress during dry storage is too low to precipitate radial hydrides. The simulations indicate that the cladding stress during dry storage is too low to cause the precipitation of radial hydrides. An important outcome of the dry storage simulations is that, when the maximum cladding temperature is 200 °C, hydrogen remains in the inner part of the cladding substrate because hydrogen diffusion is too slow to observe significant migration into the liner as shown in Figure 2.

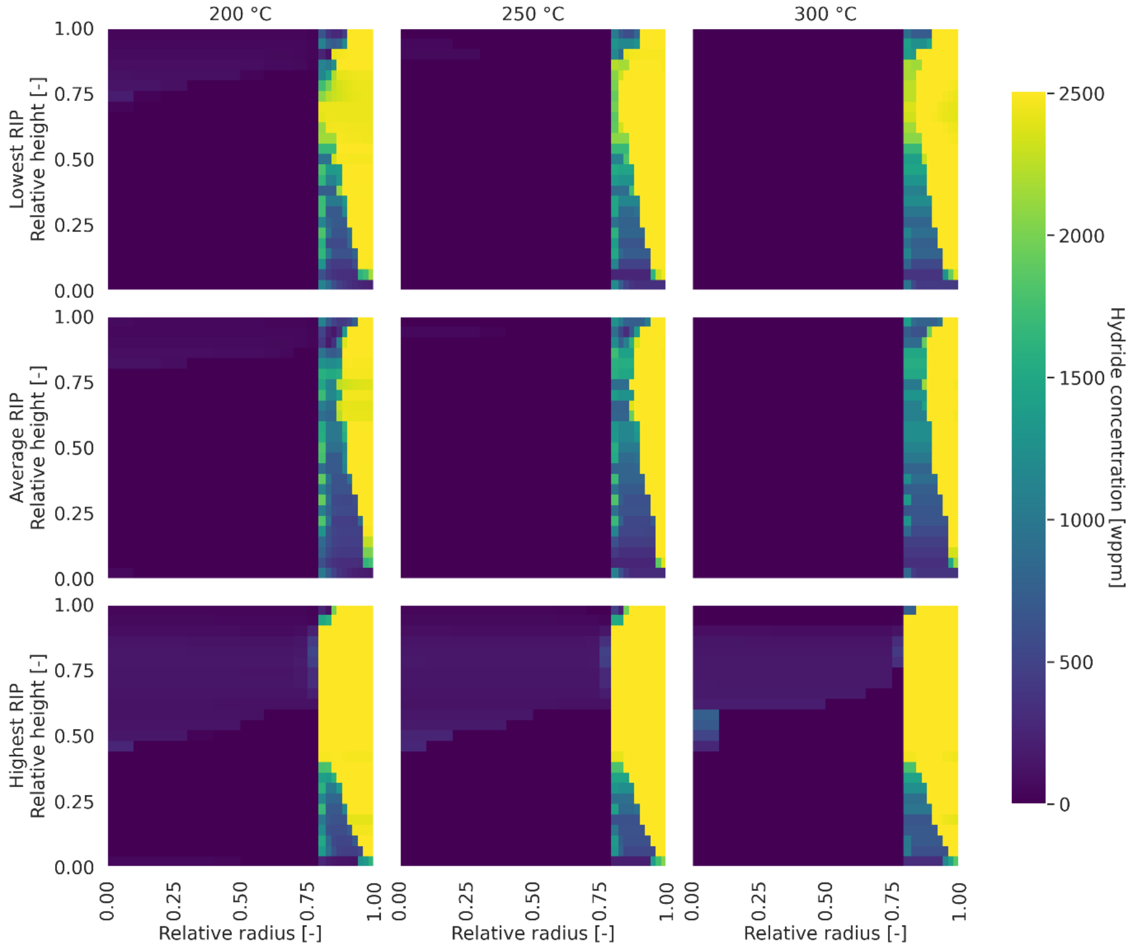

Fig. 2: Distribution of hydrides calculated at the end of dry storage

Left column: maximum dry storage temperature 200 °C; middle column: maximum dry storage temperature 250 °C; right column: maximum dry storage temperature 300 °C. Top row: Lowest RIP; middle row: Average RIP; bottom row: Highest RIP.

2.13 Spent Fuel Integrity, Regulator´s Perspective and Activities in Switzerland

Jiri Dus

Eidgenössisches Nuklearsicherheitsinspektorat (ENSI), Schweiz

Abstract

Swiss regulatory body in Switzerland ENSI presents a summary of the legal and regulatory framework governing the interim storage of spent nuclear fuel (SNF) in Switzerland, with an emphasis on the requirement for fuel rod integrity. Complementing previous Swiss presentations on dry storage, it reflects on selected insights concerning degradation mechanisms relevant to SNF safety during storage. ENSI's research and oversight activities, including the DRYstars and Z88-ENSI projects and their role in modeling and evaluating fuel performance in both operational and post-operational phases are highlighted.

1. Introduction

The fundamental principles of nuclear technology and safety are built on the concept of multiple independent and redundant barriers to the release of radioactive materials. Among these, the fuel rod (cladding and contained fuel) is the first and most essential barrier. It remains integral from the reactor core through interim storage and ultimately to disposal in a deep geological repository (DGR).

These barriers are safeguarded through a defense-in-depth strategy, implemented across different safety levels. Each level defines specific safety functions and performance limits. Through deterministic safety analyses, various initiating events and scenarios – including accidents – are evaluated to demonstrate compliance with these limits.

Noteworthy, Switzerland's Nuclear Energy Act mandates that all reasonable and appropriate measures must be taken - based on operational experience and the current state of science and technology - to protect people and the environment from harm caused by nuclear energy.

2. Legal and Regulatory Framework

In Switzerland, SNF is stored in both wet and dry interim storage facilities and subject to two primary regulatory domains: transportation and facility-based.

The transportation of SNF is regulated by international safety standards (IAEA SSR-6) and legally binding regulations such as mainly the European Agreement concerning the International Carriage of Dangerous Goods by Road (ADR). The fuel rod integrity is not directly mandated but is considered a critical input parameter for safety analyses under both normal and accident conditions.

Transport conditions are assessed through a deterministic framework that includes normal operation and hypothetical accident scenarios, such as 9-meter drop, puncture drop, thermal exposure (fire), and immersion tests.

At the national level, SNF storage in facilities is governed by the Nuclear Energy Act, the Radiation Protection Act, and associated ordinances. These are further elaborated through ENSI guidelines, such as ENSI-G05 and ENSI-G20, which provide technical expectations for storage design and fuel handling.

Three classes of nuclear installations are distinguished, nuclear power plants (NPP), other nuclear installations and DGR. NPP require the most robust safety provisions, including those for active systems, and must account for internal, external, and natural hazards. They are subject to defined exposure limits and technical criteria, including explicit requirements for barrier integrities. Fuel rod integrity must be maintained for events with frequency up to 1.0E-4 per year (see Ordinance 732.112.2).

In contrast, other nuclear facilities – such as interim storage – must consider same hazards and fulfill same dose limits but are not legally required to maintain specific barrier integrity per se. Instead, fuel rod integrity in these contexts is primarily required by ENSI documents.

Guideline ENSI-G05 focuses on the design and manufacture of dry storage casks. It mandates tests conditions and criteria based on underlaying events divided upon their site dependent frequency. Accordingly, the fuel rod and any encapsulated fuel must maintain their integrity for tests/events with frequency up to 1.0E-2 per year. Thermal criteria – such as maximum allowable cladding temperatures (local maximum and rod axial distribution) – are also required at these levels.

Guideline ENSI-G20 addresses primarily fuel and reactor performance, stipulates interim storage as well. Within the disposal concept, it requires among other parameters continued fuel rod integrity. Since design or operational changes to the fuel affect its post-reactor performance, this dependence is reflected in the same guide ENSI-G20.

Multiple stakeholders are involved in the SNF management process, with nuclear NPP operators playing a central role. They define fuel parameters, manage both operational and storage conditions, and initiate licensing requests for transportation.

The cask vendors submit license applications at the NPP's request and stay in direct contact with ENSI, however, NPP determines fuel characteristics that affect safety demonstrations. These characteristics may be subject to a prior evaluation by ENSI to facilitate the lengthy and complex licensing process.

3. Fuel Degradation Mechanisms

The behavior of fuel rods during long-term storage is influenced by multiple parameters, with temperature being particularly important. Degradation mechanisms can affect fuel rod integrity directly or impair mechanical properties needed to withstand operational and accidental loads.

Thermal creep is well-characterized for non-irradiated cladding and, increasingly, for irradiated cladding on so called defueled samples. For example, CWSR Zry-4 creep behavior under dry storage conditions described in [1], provides an applicable model to dry interim storage. Swiss storage analyses typically apply a 1 % cladding elongation limit. This conservative value has been kept to cover unknown phenomena especially in high burn-up fuel. As recently demonstrated in [2], developed fuel-cladding bonding limits hoop stress and suppresses hydride reorientation on one hand, may provoke radial hydrides at the locations of fuel cracks on the other hand. To better understand the bonding effect on fuel rod behavior during interim storage, more creep examinations with fuel inside should be internationally pursued.

Hydride formation and reorientation remain significant concerns due to their impact on cladding mechanical performance. In [3] EPRI reviewed 20 years of data and concluded that radial hydrides, while not necessarily a mechanism causing cladding failure directly, require robust cask design to maintain safety equally to fuel rods without hydride reorientation. NRC confirmed in NUREG-2224 [4] that rods with high radial hydride fractions in Zry-4 showed comparable mechanical capacity to unaffected rods, thereby justifying cladding-based safety assessments. These findings should have been reinforced by recent U.S. DOE tests for other alloys like M5 or ZIRLO [5], [6], however, the low fuel rod internal pressure didn't cause remarkable hydride reorientation. Moreover, the absence of possible pellet-cladding mechanical interaction – coming from He driven fuel swelling – in any of these tests raises questions about their representativeness for prolonged storage and subsequent transportation. Helium-induced swelling of fuel may lead to increased hoop stress in the cladding during storage. Modeling of these stresses has been developed [7], and applied [8], recognizing that swelling would saturate within the first 100 years of storage. Evaluation of these models and predictions remains a topic for further analyses, ideally supported by measurements of long-stored fuel even under wet conditions where fuel swell must be active as well.

Hydrogen behavior and redistribution, especially in duplex cladding, have also been studied at PSI using advanced imaging techniques, e.g. [9]. The role of liners, such as in Zry-2 claddings, has been shown to localize hydride formation under certain conditions relevant for dry storage and improve ductility of cladding overall [10], [11].

4. ENSI's Activities and Research Commitments

The safe reactor operation belongs to the highest priority of ENSI´s oversight ensuring sound fuel at the end-of-life (EOL) conditions. Swiss NPP´s continuous participation in diverse in-pile and out-of-pile performance programs including post irradiation examinations in hot cells, fuel health inspections and own driven research activities have been required and acknowledged by ENSI on the way to high fuel burn-up. With the imperative to keep highest possible level of safety stipulated by the nuclear energy act, state-of-the-art and best possibly validated fuel performance codes are in place to calculate the EOL fuel conditions by vendors analyses. Even if the liner-claddings have not been developed to ensure cladding performance during and after interim storage, they play an important role in the overall safety assessment. Therefore, many research activities have been initiated by Swiss NPPs and closely watched by ENSI to investigate the hydrogen diffusion as the underlying phenomenon.

In terms of independent safety evaluation of fuel interim storage ENSI relies on three pillars. The first one being the co-sponsorship of national or international research (e.g. SCIP, HELP), second the initiation and funding of the DRYstars numerical project at PSI, and lastly the participation in dedicated international working groups and meetings, e.g. SFERA (IAEA), ESCP (EPRI) and SEDS-Workshop (GRS).

Within the DRYstars the Falcon code has been expanded by storage specific models for thermal cladding creep and fuel swelling [12]. To properly capture the Hydrogen kinetics in liner claddings, HYPE module has been developed [13] and loosely coupled to Falcon. With such calculations, hydride related issues such as delayed hydride cracking or hydride reorientation can be evaluated with specific failure models.

In the currently beginning Phase 3 of DRYstars, pin-by-pin statistical evaluations, leveraging machine learning to assess complex phenomena without clear bounding cases, such as gap closure and PCMI-DHC interactions are envisaged. The goal is to establish a basis for advanced accident scenarios in reactor with the associated project STARS at PSI in parallel. Focus should be given also on identifying alternative, computationally faster fuel codes applicable to MOX fuel.

To close the numerical evaluation scheme in dry storage casks, the computations of fuel assembly decay heat, and thermal analyses of dry cask up to the fuel rod level have been developed. In this regard, ENSI supports thermal modeling research in collaboration with the University of Bayreuth using customized FEM solver Z88-ENSI V3 [14]. The validated semi-analytical boundary condition at the basket-cask-body-gap saves computational effort and facilities reliable thermal assessments with standard office computers.

References

[1] Cappelaere, C., et al. (2011). A Robust Model To Describe The Thermal Creep Of CWSR Zircaloy 4 Cladding For Fuel Cycle Back-end Application. TopFuel.

[2] Andersson, R. K., et al. (2024). On The Effects Of The Pellet On Thermal Creep And Hydride Reorientation During Dry Storage Conditions. TopFuel.

[3] Waldrop, K. (2020). Effect of Hydride Reorientation in Spent Fuel Cladding - Status from Twenty Years of Research. EPRI 3002016033.

[4] NRC (2020). NUREG-2224: Dry Storage and Transportation of High Burnup Spent Nuclear Fuel.

[5] Bignell, J., et al. (2024). High-Burnup Spent Fuel Data Project Sibling Pin Test Campaign Closeout and Summary Report. DOE Report SAND2024-16441R.

[6] Billone, M., et al. (2020). Preliminary Destructive Examination Results for Sibling Pin Cladding. ANL-19/53 Rev. 2.

[7] Raynaud, P., & Einziger, R. (2015). Cladding stress during extended storage of high burnup spent nuclear fuel. Journal of Nuclear Materials.

[8] Sonnenburg, H.-G., & Bolt, F. (2017). Brennstabverhalten im Normalbetrieb, bei Störfällen und bei Langzeitlagerung. GRS 464.

[9] Gong, W., et al. (2019). Hydrogen diffusion and precipitation in duplex zirconium nuclear fuel cladding quantified by high-resolution neutron imaging. Journal of Nuclear Materials.

[10] Duarte, L., et al. (2021). Effect of the inner liner on the hydrogen distribution of zircaloy-2 nuclear fuel claddings. Journal of Nuclear Materials.

[11] Konarski, P., et al. (2023). Modeling of hydrogen behavior in liner claddings. Journal of Nuclear Materials.

[12] Konarski, P., et al. (2021). Spent nuclear fuel in dry storage conditions – current trends in fuel performance modeling. Journal of Nuclear Materials.

[13] Konarski, P., et al. (2024). Development and testing of the hydrogen behavior tool for Falcon – HYPE. Nuclear Engineering and Technology.

[14] Nimmesgern, J. (2023). Accelerated Determination Of Three-dimensional Temperature Fields of Dual-purpose Casks Using Combined Numerical And Analytical Methods. PATRAM.

2.14 Extended Storage of Spent Nuclear Fuel in Casks - Recent Developments at TÜV NORD

Gerold Spykman

TÜV NORD EnSys GmbH & Co.KG, Germany

Extended abstract

In the previous SEDS meetings in 2023 [4] and 2024 [5] we presented preliminary results of our work on the inventory assessment of spent nuclear fuel in casks during an extended storage time with fuel rod performance codes. Within this extended abstract we summarize the developments since the last SEDS meeting in 2024.

The aim of this project is to establish methods and a prototype tool to access fuel performance in dry cask for a prolonged storage time up to 100 years and longer. So far, we have explored current assessment methods for fuel performance during dry storage and analyzed possible future approaches (see [4] and [5] for details). In the current stage of the project, we focus primarily on the handling of uncertainties and the conservatism of underlying assumptions. This is vital in order to meet the guidelines in the ESK position paper on extended storage [6] that the safety-related verification should be based on a protection-goal-oriented approach. Further points in the ESK-paper include knowledge retention and data availability. As before, we are addressing these issues with the fuel performance code TRANSURANUS [1], [2] with an adapted input generation desk and our own spent fuel database TITANIA [3].

Throughout the work on the prototype, we have gained the following new insights:

- Fuel assembly rotation orientation in the cask compartment is not documented
- Decay power data is calculated in a conservative manner to a reference date that differs from the loading date for the FA and not for the single pins
- If best-estimate values and uncertainties of data are not available these parameters have to be evaluated as fixed parameters, which poses another challenge

Since the last SEDS meeting in 2024 we have reached the following new milestones:

- Some probabilistic based calculations show strong dependencies between input parameters and results that are important for long-time cladding performance under storage conditions
- Implementation of Pearson correlation coefficient and Spearman ranging to facilitate sensitivity analyses of input and model parameter
- Implementation of test procedures (e.g. t-tests) on statistical significance of the calculated correlation coefficients (in progress)
- Up to now correlations coefficients and rankings are determined at fixed times (end of in-pile life, end of drying procedure or end of dry storage period), correlation over the complete timeline will be needed for further analysis (in progress)
- At present, the disk space requirements and the computing time needed for the statistical timeline analysis are being determined and initial calculations are being carried out.
- Large data storage capabilities are needed for fast access and propriate visualization: an improvement of the visual data management tool will be necessary.

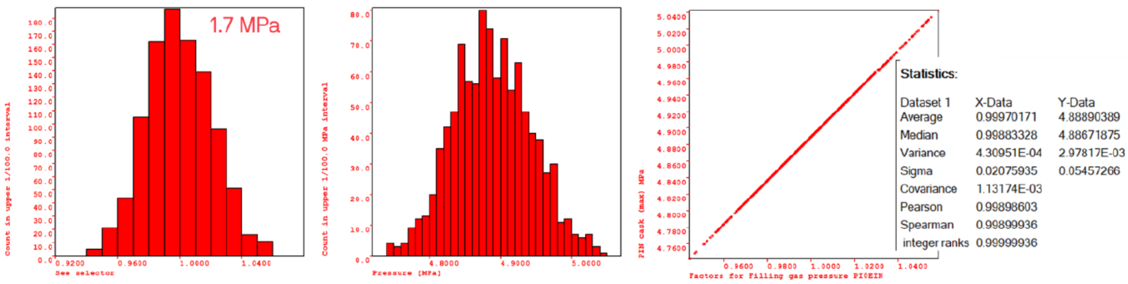

Fig. 1: Variation of the initial fuel rod filling gas pressure for 1000 input desks

Input distribution (left) - max. fuel rod inner pressure during storage (middle) - scatter plot with correlation and ranking data tableau (right) (© TÜV NORD EnSys GmbH Co.KG)

In order to determine the sensitivity of the result on the input parameters we carried out many calculations with varying input parameters as described in our paper from 2024 [5]. Furthermore, we implemented new tools in our prototype to calculate the Pearson correlation coefficients and the Spearman ranking in order to obtain a measure on the dependency of input variation and output distribution.

An example of these analyses is shown in Figure 1. In this example, one of several test calculations carried out so far, the initial fuel rod filling gas pressure was varied 1000 times by dicing values from the specified distribution for the input parameter. The input distribution is constructed from the specified manufacturing nominal, minimal and maximally allowed values. As one would expect a higher initial inner pressure results in a higher inner fuel rod pressure after irradiation with a Pearson correlation coefficient and a Spearman ranking value close to one.

The correlation for the other input parameters, which we analyzed, do also fit within the expected frame of physical dependencies. All these results are in an expected frame following the theory and physical dependencies. However, some results show a strong dependency but a very small variation of the output parameter e.g. with a bandwidth in the order of one mbar. In these cases, there might be a numerical dependency from the code but only a negligible physical one. This must be further investigated with appropriate test procedures like the t-test method on statistical significance.

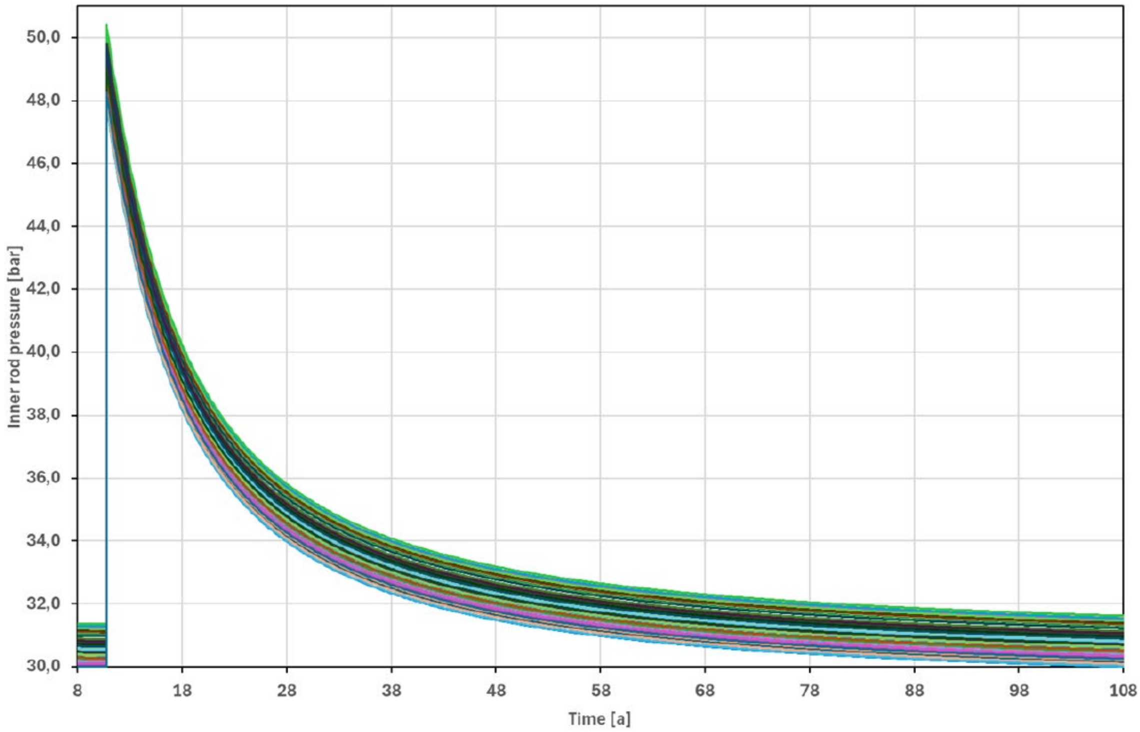

Fig. 2: Dependence of the inner rod pressure over time on the initial filling gas pressure for a set of 100 variations (© TÜV NORD EnSys GmbH Co.KG)

In Figure 1 we presented a result at one point in time, here the maximum pressure during storage which occurs close after loading time due to the highest rod temperatures. But this is only a snapshot in time, and we must investigate whether this result is valid for the complete timeline or not. As a first test, we calculated the time dependent inner rod pressure for 100 variations of the initial filling gas pressure with the same input distributions parameter as shown in Figure 1. In Fgure 2 we plotted the calculated histories of the inner rod pressure that show the slope and variations. The preliminary results also indicate that:

- the Pearson correlation coefficient is varying over time during in-pile life and is lower than expected, which must be investigated further,
- the Spearman ranking and the integer ranking method give nearly constant values close to one as expected, and that
- the influence of the time step control of the code within this method must be investigated.

In conclusion, we have made important progress in extending the prototype for input and output processing by implementing the Pearson correlation coefficient method and the Spearman ranking. This will be continued by implementing statistical tests on significancy accompanied by other improvements and many calculations.

References

[1] K. Lassmann TRANSURANUS: a fuel rod analysis code ready for use Journal of Nuclear Materials 188 (1992), 295 – 302.

[2] P. Van Uffelen, Cs. Győri, A. Schubert, J. van de Laar, Z. Hozer, G. Spykman Extending the application range of a fuel performance code from normal operating to design basis accident conditions Journal of Nuclear Materials, 383 (2008), 137 – 143.

[3] TÜV NORD EnSys Hannover GmbH & Co. KG TITANIA Data Management System for Full Core LOCA Analysis using TRANSURANUS AESJ Water Reactor Fuel Performance Meeting 2005, Kyoto, Japan.

[4] Extended Storage of Spent Nuclear Fuel in Casks Inventory Assessment using Fuel Rod Performance Codes Gerold Spykman, TÜV NORD EnSys GmbH & Co.KG Presentation at SEDS in May 2024 at GRS in Garching, Munich.

[5] Extended Storage of Spent Nuclear Fuel in Casks Inventory Assessment using Fuel Rod Performance Codes – An update and recent developments Gerold Spykman, TÜV NORD EnSys GmbH & Co.KG Presentation at SEDS in May 2023 at GRS in Garching, Munich.

[6] Entsorgungskommission – ESK Verlängerte Zwischenlagerung bestrahlter Brennelemente und sonstiger hochradioaktiver Abfälle in Abhängigkeit von der Auswahl des Endlagerstandorts Positionspapier vom 23.03.2023 https://www.entsorgungskommission.de/sites/default/files/reports/ESK_Positionspapier_verlaengerte_ZL_40plus_ESK105_23032023.pdf.

2.15 Dry Storage Facility in Dukovany NPP

Jiri Gerza, Dominik Král

NPP Dukovany, Czech Republic

The paper presented by Dukovany NPP has the following parts:

The first part describes the history of dry spent fuel storage facility at Dukovany NPP based on the dual-purpose metal cask and the actual situation regarding the cask operation license.

The second part is focused on the general approach to the aging management (AM) of the plant technology and the new implementation of AM program onto the casks. Besides the preventive maintenance and periodical checks, a supporting experimental program is being prepared, mostly focused on the metal gaskets as the most sensitive part.

In the third part, a set of calculation analyses is presented. The analyses cover several degradation mechanisms acting on the cask materials with a potential impact on the cask lifetime. The example of the result of the radiation effect analyses is shown.

2.16 Experience and Challenges from 60 years of Dry Storage of Metallic Uranium Research Reactor Spent Fuel

Peter Bennett

Norwegian Nuclear Decommissioning (NND)

N/A

2.17 Generic Cask Modelling Options to promote both Exchange and Comparability and their Illustration using a Muographic Application

T. Braunroth and K. Arnswald

Gesellschaft für Anlagen – und Reaktorsicherheit (GRS) gGmbH, Germany

M. Wagner

Helmholtz Zentrum Dresden Rossendorf (HZDR), Germany

Introduction and Motivation

Muography describes the non-destructive imaging of objects and hidden or covered structures by using muons. Currently, the vast majority of muographic applications exploit *atmospheric muons*, i.e. muons that are produced in the atmosphere due to interactions of the primary cosmic radiation with atmospheric particles.

First muographic applications already took place more than 50 years ago. An example that is often cited (although it was not the first application) is the identification and localization of hidden chambers in the Great Pyramids by Alvarez and colleagues /ALV 70/. Since then, the field of applications has increased continuously, including geological studies (such as the imaging of volcanos /TAN 19/) or applications in conventional industry (such as blast furnace imaging /VAN 19/). Nowadays, there's also a great interest in using muography for inspections of the public infrastructure. In addition, there are also multiple examples for the use of muography in the nuclear sector, including the imaging of the damaged reactor Fukushima Daiichi Unit-1 /FUJ 20/ and the imaging of the G2 reactor in France /PRO 23/. Muography is seen as a promising method with various applications in the nuclear field which is further highlighted by a dedicated IAEA TECDOC /IAEA 22/.

A particular application that has received substantial interest for the past decades is the non-destructive imaging of storage/dual-purpose casks and their interiors, including spent nuclear fuel. A strong driver for this interest is the increasing need for non-destructive examination methods due to extended interim-storage periods in many countries. Various numerical studies have been performed so far which indicate that an identification of vacant fuel-element slots (missing fuel assemblies) and smaller structures (down to the level of a fuel rod) are possible /POU 17, BRA 21/. However, there is a direct correlation between resolution and the number of required events to achieve this resolution, which can lead to very long measurement times. While in-field measurements are still sparse, some of these findings mentioned above have already been experimentally observed but also indicate practical obstacles /BON 24/.

In comparison, muography can still be seen as a rather new method. There are many opportunities for improvements, including the development of advanced detection systems, the development of advanced image reconstruction methods and extended numerical studies to perform feasibility studies and to evaluate the benefits of potential optimizations. In addition, extended test- and field measurements are required to achieve substantial validation and to identify practical obstacles. Both from an international as well as a national perspective, the muographic communities are rather small and have therefore limited capacities. Currently, potential synergies, e.g. by sharing not only results but also in-depth information (including information on the applied cask model), are often not fully exploited.

Generic cask modelling to address uncertainties and to support collaboration

The results of numerical studies are always correlated to the applied assumptions, e.g. in terms of the adopted geometry. Even for well-established dual-purpose casks (DPC) such as the CASTOR® V/19, precise, unambiguous and complete geometry descriptions are not publicly available. Developers of such casks are – understandably – cautious to share information (intellectual property). Consequently, code developers and users of numerical studies usually use different cask models and are equally cautious to share associated information, especially with increasing level of detail. This limited access to information is a key barrier and reduces both comparability and transparency.

Generic cask models that mimic features of a real cask can solve some of these issues but usually suffer from a reduced interest due to an apparent lack of significance. However, due to potential benefits for fostering cooperation and exploiting synergies, GRS and HZDR developed a set of three generic models following the DPC CASTOR® V/19 that can potentially be shared with the interested community. Furthermore, this model already supports the topical exchange of information between GRS and HZDR.

The basic idea is to have a generic model that mimics publicly available basic properties of the DPC CASTOR® V/19 (“Model R”). Two additional models (labeled “Model O” and “Model C”) represent – from a muographic perspective – extremal variations of Model R, leading to optimistic (Model O) and conservative (Model C) results. To some extent, this approach provides insights into associated systematic uncertainties – an aspect that is usually not well addressed in recent numerical studies. Moreover, it is expected that simulations using a realistic CASTOR® V/19 model will lead to results that are within the limits set by Model O and Model C (see Fig. 1).

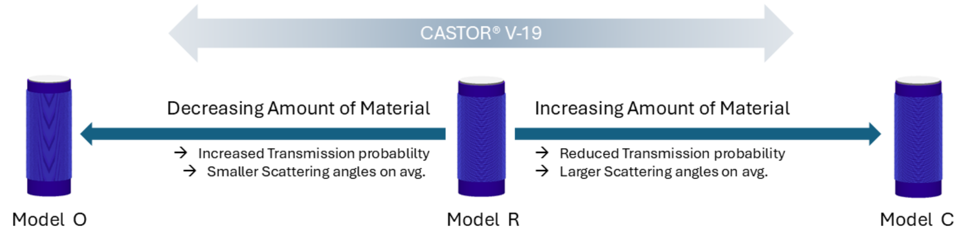

Fig. 1: Sketch of the generic models and the expected link to the CASTOR® V/19

The Models R, C and O are modular and consist of multiple components, such as various kinds of lids, absorption rods, basket and fuel assemblies (see Fig. 2). The height varies between 585 cm (O) and 599 cm (C), the outer diameter varies between 230 cm (O) and 260 cm (C). Consequently, also the mass (without fuel assemblies) varies between 80 Mg (O) and 128 Mg (C). For comparison: CASTOR® V/19 has a height of 594 cm, an outer diameter of 244 cm and a mass of 108 Mg /GNS 23/.

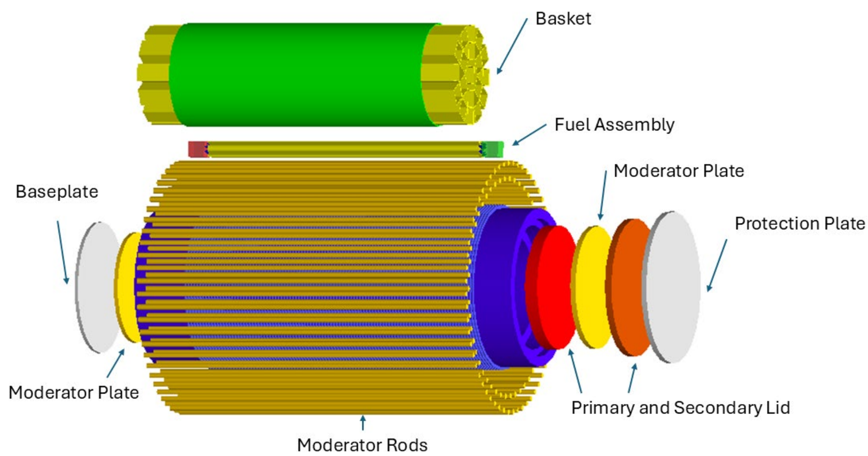

Fig. 2: Explosion drawing of model R

On the basis of these three models, GRS applied GEANT4 to perform muographic Monte-Carlo simulations using monoenergetic muons. Some results comprising the median of the effective scattering angle are shown in Figure 3. It is obvious, that the contrast of the images is correlated to the incoming muon energy. As expected, there is also a systematic trend toward larger (smaller) scattering angles for Model C (Model O) compared to Model R.

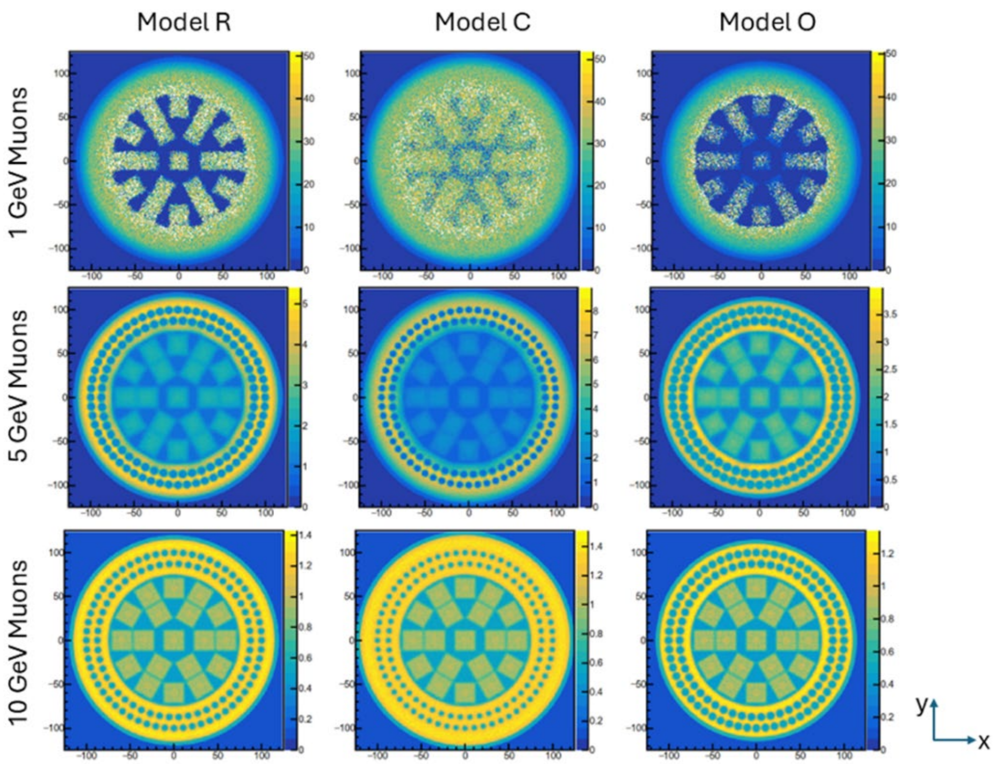

Fig. 3: Simulated results showing the median of the effective scattering angle (colour coded in degree) for 1 GeV (top), 5 GeV (centre) and 10 GeV (bottom) for the geometry of model R (left), model C (middle) and model O (right)

In comparison to Model R, Model C leads to larger scattering angles on average (+19 % for 10 GeV and +43 % for 1 GeV), while Model O leads to smaller scattering angles on average (-18 % for 10 GeV and -28 % for 1 GeV).

In addition, HZDR also performed similar simulations using the Monte-Carlo Code G4Beamline for the Model R. A comparison of the results is shown in Fig. 4. For structures within the basket the agreement is very good. Deviations increase towards the outer regions which can be traced back to different dimensions of the outgoing detector surface.

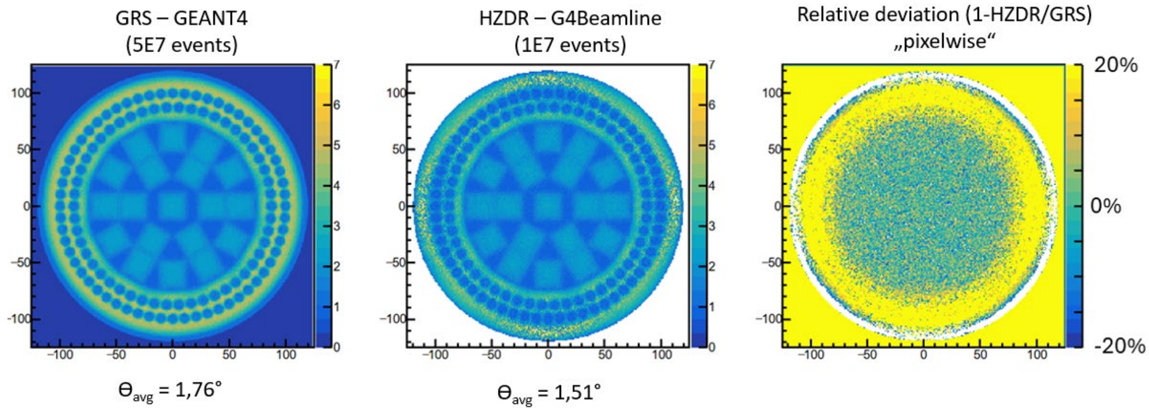

Fig. 4: Comparison of simulated results for 5 GeV Muons and the cask geometry Model R

Left: Results of the GEANT4 simulation. Centre: Results of the G4Beamline simulation. Right: Relative Deviations between the GEANT4 and G4Beamline simulations.

Summary and Outlook

Presently, the international and trans-organisational exchange focuses on sharing results and less on sharing basic information and data – this is also true for the muographic community. This can lead to challenges when it comes to reproducing results or validation. In addition, resources are limited, it is therefore recommended to cooperate and to use synergies as much as possible. The current practice, however, is different: Most of the actors currently investigating the potential use of muography for examining DPC use their own simulations, geometries and tools for analysis. Not only does this complicate the comparison of results, it also can lead to inefficiencies along the process. For example, advanced and iterative image reconstruction algorithms can be challenging – translating them into an efficient code (e.g. in terms of computation time and memory load) requires certain skills and qualifications, which naturally not every actor can provide. If such code with the right interfaces is available already, a possibly bad “reinvention of the wheel” is not required. Sharing such information would also allow to reduce barriers for new actors. For example, current R&D activities investigate compact anthropogenic muon sources [10] with a significantly higher muon flux compared to the atmospheric muon spectrum – from the perspective of an extended interim storage, such a system might be a game changer. Giving those developers access to the tools and information might help to collect associated R&D funding more efficiently.

The applied cask model within numerical studies is of paramount importance when it comes to the interpretation of the simulated results – usually neither the Monte-Carlo code nor the cask geometry are shared with externals without restrictions. This present contribution focused on a generic model that can be shared with the community without specific restrictions. It should be seen as a first attempt to foster cooperation: Both partners are currently evaluating additional steps which might cover the sharing of code, the sharing of simulated/experimental data or the organization of topical workshops to bring the community closer together.

Acknowledgement

This GRS research was funded by the Federal Ministry for the Environment in Germany under Contract 4723E03290.

References

[1] L.W. Alvarez et al: Search for Hidden Chambers in the Pyramids. Science 167, 832 – 839 (1970).

[2] G. Bonomi et al: Muon Tomography for Reverification of Spent Fuel Casks (the MUTOMCA Project). Journal of Advance Instrumentation in Science 2024, no. 1 (2024).

[3] T. Braunroth et al: Muon radiography to visualize individual fue rods in sealed casks, EPJ Nuclear Sci. Technol. 7, 12 (2021).

[4] H. Fujii et al: Investigation of the Unit-1 nuclear reactor of Fukushima Daiichi by cosmic muon radiography. Prog. Theor. Exp. Phys. 2020, 043C02 (2020).

[5] GNS Gesellschaft für Nuklear-Service mbH: CASTOR® V/19 (Product Information). 10/2023.

[6] IAEA: Muon Imaging – Present Status and Emerging Applications, 2022.

[7] D. Pulson et al.: Cosmic ray muon computed tomography of spent nuclear fuel in dry storage casks, Nucl. Instr. Meth. A 842, 48 (2017).

[8] S. Procureur et al: 3D imaging of a nuclear reactor using muography measurements. Sci. Adv. 9, eabq8431 (2023).

[9] P. Shukla and S. Sankrith: Energy and angular distribution of atmospheric muons at the Earth. arXiv:1606.069707v3.

[10] H. K.M. Tanaka: Japanese volcanoes visualized with muography. Philosophical Transactions A 377, 2018042 (2019).

[11] D. Terzani et al: Measurement of directional muon beams generated at the Berkeley Lab Laser Accelerator. arXiv:2411.02321.

[12] S. Vanini et al: Muography of different structures using muon scattering and absorption algorithms. Philosophical Transactions A 377, 2018051 (2019).

2.18 Non-invasive Imaging of Transport and Storage Casks

M. Wagner

Helmholtz Zentrum Dresden Rossendorf (HZDR), Germany

N/A

2.19 On the Applicability of the Master Curve Concept for Ductile Cast Iron based on Experimental and Microstructural Results

<u>*Marcel Holzwarth*</u>

PhD student, Materials Testing Institute University of Stuttgart (MPA), Stuttgart, Germany

Wolfram Baer

PhD, Federal Institute for Materials Research and Testing (BAM), Berlin, Germany

Uwe Mayer

Dipl.-Phys., Materials Testing Institute University of Stuttgart (MPA), Stuttgart, Germany

Stefan Weihe

Professor, Materials Testing Institute University of Stuttgart (MPA), Stuttgart, Germany

Introduction

Based on the state-of-the-art research and regulations, the application of the fracture mechanics master curve (MC) concept to ferritic ductile cast iron (DCI) is being investigated in a joint research project (MCGUSS) between MPA Stuttgart and BAM Berlin.

According to the IAEA (2012), the safety assessment of DCI containers for transport as well as interim and final storage of radioactive materials is based on the fracture mechanics criterion of general exclusion of crack initiation. In addition, a safety assessment for dynamic loading is explicitly required by the ASME Code (2019). The MC concept is currently used as a supplement to the established deterministic ASME reference curve concept and allows an effective statistical consideration of the scatter of the material toughness in the transition regime and it is currently the only established standardized method to consider brittle fracture in the ductile-to-brittle transition regime. However, for DCI, a systematic review of potential modifications to the assumptions and the procedure according to ASTM (2024) and an associated validation are still lacking. Therefore, a methodology shall be established to determine and assess dynamic fracture toughness values of DCI in the ductile-to-brittle transition regime using test specimens extracted from a component.

Test Material Specification and Characterization

The experimental program uses a DCI material of grade GJS-400 (formerly known as GGG-40), which is commonly used for transport and storage containers for radioactive materials. Twelve cast blocks with dimensions of 820x1550x300 mm were produced just for use in this project. To avoid batch effects, this was done in a single casting. The tailored manufacturing specification for these cast blocks aimed to produce a homogeneous DCI material close to that used for nuclear transport and storage containers. Figure 1 shows a schematic of the cast blocks. For ease of handling, 2 smaller blocks (①+②) were extracted from each main block, which will form the basis for the SE(B)140 specimens and the extraction of smaller specimens.

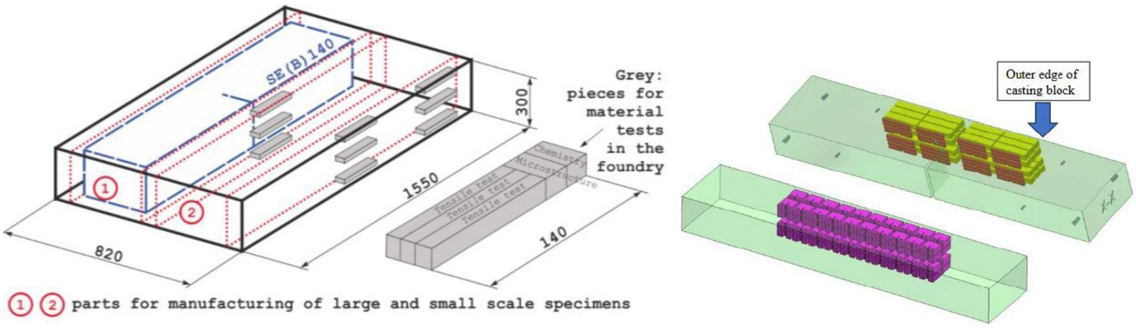

Fig. 1: Left: Schematic of the GJS400 casting blocks; Right: 2 examples of extraction plans for C(T)25 and SE(B)

Experimental Program

The experimental program included a basic mechanical-technological material characterization consisting of tensile, Charpy and Pellini tests. To determine the relevant loading rate for brittle fracture, instrumented C(T)25 fracture tests were performed at different loading rates at a temperature of -40 °C. The relevant loading rates are $5x10^3$ MPa$\sqrt{m}$s^{-1} and $5x10^4$ MPa$\sqrt{m}$s^{-1}. In order to later transfer the relevant loading rate to other specimen sizes or shapes, the time-dependent course of the Weibull stress is evaluated by numerical analysis. With this information a series of dynamic fracture tests consisting of DC(T)9, C(T)25 and C(T)50 specimens were performed at MPA.

BAM performed corresponding test series with SE(B)10 (pre-cracked Charpy), SE(B)25 and SE(B)140 specimens to cover the influence of specimen geometry. In total about 400 tests were performed during this project.

The experimental program is complemented by extensive fractographic and metallographic studies using scanning electron microscopy and cross sectioning, as well as characterizations of the chemical composition of the material and of the geometry and distribution of the graphite particles.

Results

$K_{Jc,d}$ values were evaluated for all C(T)25 specimens and some C(T)50 and DC(T)9 specimens. Figure 2 shows the $K_{Jc,d}$ values for these tests and the SE(B) tests performed by BAM. Furthermore, Figure 3 shows the standard Master Curve evaluation according to ASTM E1921 for the C(T)25 test results and a first attempt to modify the Master Curve by changing the coefficient from 0.019 to 0.045. This modification requires further validation and is only one of many possible modifications.

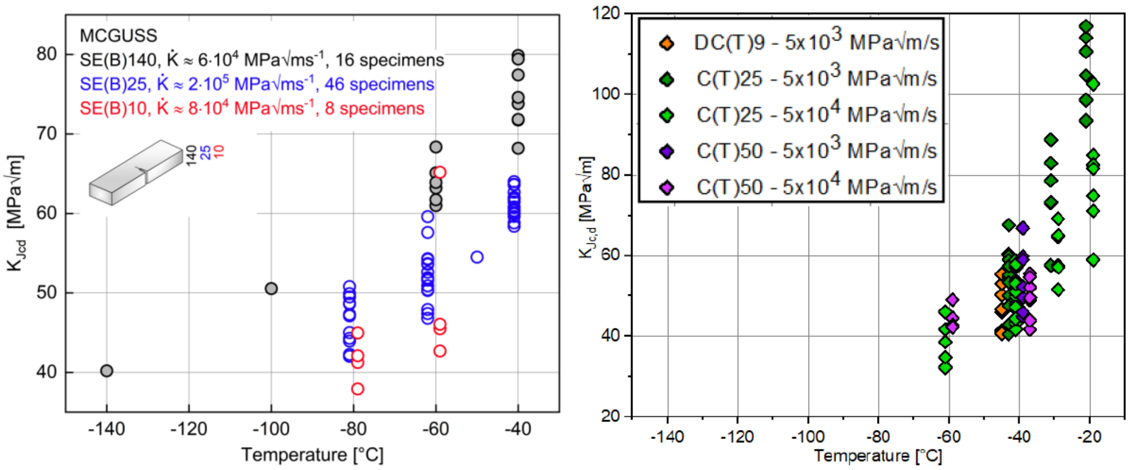

Fig. 2: $K_{Jc,d}$-Values for the conducted C(T) and SE(B) test series at different temperatures and loading rates

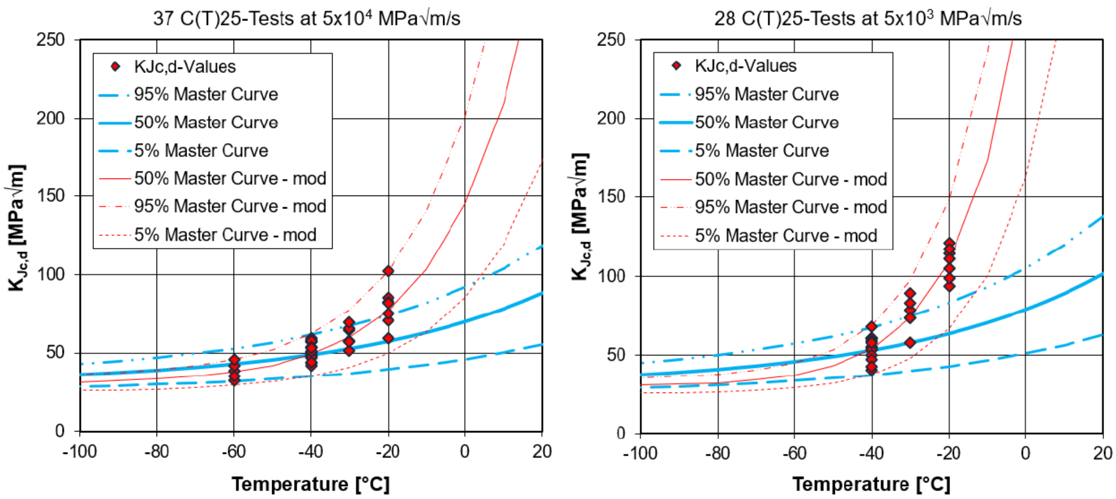

Fig. 3: Standard Master Curve evaluation according to ASTM (2024) (blue) and modified Master Curve (red)

The SE(B) specimen results clearly show an inverse size effect. This does not correlate with the weakest link effect attributed to steels which dictates lower fracture toughness values for larger specimens. Due to the presence of graphite particles in the DCI material we currently assume that these particles play a significant role in the failure behavior of DCI materials and propose the following model: *"Specimen size-dependent arrest of local brittle failure before global brittle failure by weakest link".*

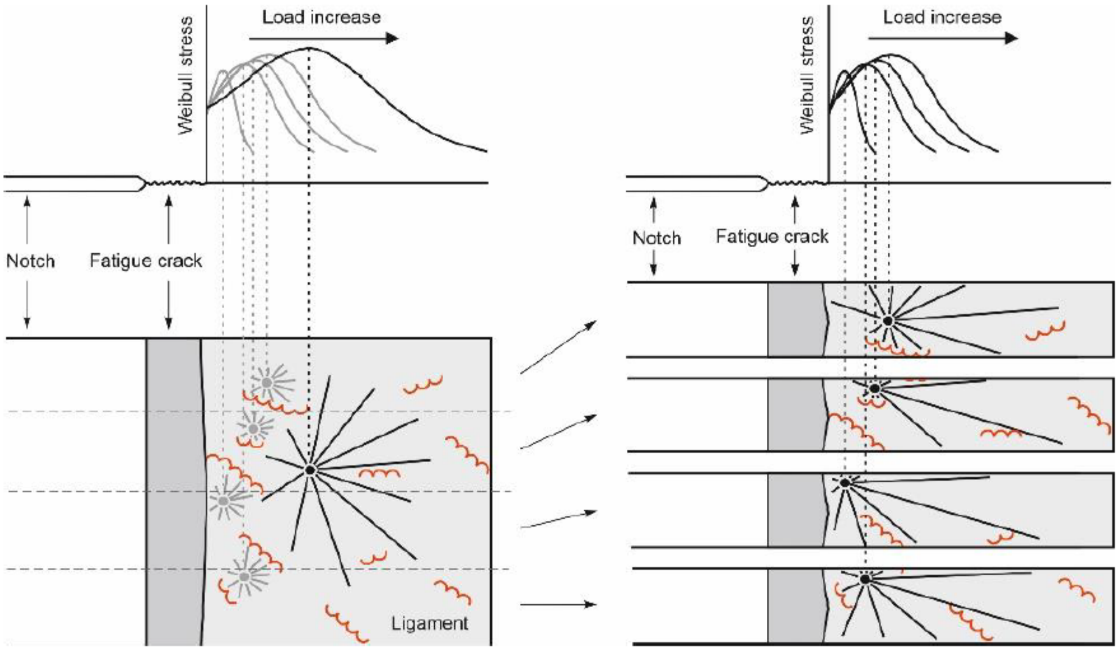

Fig 4: Model: "Specimen size-dependent arrest of local brittle failure before global brittle failure by weakest link"

Figure 4 shows a schematic of the proposed model. With increasing load, and therefore Weibull stress, various defects can initiate brittle failure. Favorably oriented graphite barriers energetically weaken the running crack and can lead to local crack arrest and in turn further increasing load. This continues until a defect without sufficient graphite barriers initiates instable fracture, leading to global failure of the specimen. Larger specimens have higher probability of possessing favorably oriented graphite barriers, thus increasing fracture toughness. Smaller specimens can still experience local crack arrest, the probability is just lower compared to larger specimens.

Summary

The overall objective of this joint research project is to investigate, further develop and provide a method for assessing the brittle fracture safety of DCI materials at increased loading rates. This should make it possible to determine dynamic fracture toughness values of DCI materials in the toughness transition range in a targeted manner using samples extracted from a component.

At this stage of the project it can be concluded that the Master Curve Concept is not applicable to DCI as it is currently described in ASTM E1921. However, it is highly likely the Master Curve Concept can be applied to DCI with appropriate modifications. To validate these modifications, further research into K_{min}, the Weibull parameters and the inversed size effect is required and will be undertaken in an upcoming research project (MCGUSS II).

Acknowledgements

The joint research project MCGUSS “Investigation of the Master Curve Concept for Ferritic Ductile Cast Iron” with the subprojects “Investigations using C(T) and DC(T) specimens”, Project No. 1501650, and “Investigations using SE(B) specimens”, Project No. 1501651, was funded by the German Federal Ministry for Environment, Nature Conservation, Nuclear Safety and Consumer Protection (BMUV) on basis of a decision by the German Bundestag.

Federal Ministry
for the Environment, Nature Conservation,
Nuclear Safety and Consumer Protection

References

[1] IAEA (2012), “Guidelines for the Safe Design of Shipping Packages against Brittle Fracture” IAEA Specific Safety Guide No. SSG-26, Advisory Material for the IAEA Regulations for the Safe Transport of Radioactive Material, Vienna, International Atomic Energy Agency, 371-389.

[2] ASME-Code (2019) “ASME Boiler & Pressure Vessel Code III, Division 3 Containments for Transportation and Storage of Spent Nuclear Fuel and High Level Radioactive Material and Waste, WC-2300 Fracture Toughness Requirements for Material”.

[3] ASTM International (2024), “Standard Test Method for Determination of Reference Temperature, T0, for Ferritic Steels in the Transition Range”, ASTM E1921-24, West Conshohocken, PA: ASTM International, appr. May 1.

2.20 Adaptive Service Life Management for Concrete Building Structures of Interim Nuclear Storage Facilities

v. Wehren, S.; Leusmann, T.

Technische Universität Braunschweig, Institute of Building Materials, Concrete Construction and Fire Safety (iBMB), Germany

Niederleithinger, E.; Oeff, J.

Bundesanstalt für Materialforschung und -prüfung (BAM), Germany

Sperbeck, S.

Gesellschaft für Anlagen- und Reaktorsicherheit (GRS) gGmbH, Germany

Corrosion protection of the reinforcing steel is a prerequisite for the durability and structural integrity of reinforced and prestressed concrete structures. Therefore, corrosion monitoring is an important component of the life cycle management of many structures exposed to atmospheric conditions or a damaging environment. This study focuses on the assessment of corrosion in concrete structures containing reinforcing or prestressing steel. A particular focus lies on the development, testing and application of calibration-free mini-sensors to detecting the corrosion initiation of reinforcing bars in concrete structures. These sensors comprise multiple thin iron wires connected in series. The main advantage is the simple design and robust measurement principle. The sensors are intended for post-installation in boreholes filled with mortar in order to serve as a basis for adaptive service life management of concrete structures, such as nuclear interim storage facilities, where high durability and long-term reliability are important. The aim of this investigation is to enable condition-orientated maintenance and safety assessment over longer operating periods of interim nuclear storage facilities.

Gesellschaft für Anlagen- und Reaktorsicherheit (GRS) gGmbH

Schwertnergasse 1
50667 Köln
Telefon +49 221 2068-0
Telefax +49 221 2068-888

Boltzmannstraße 14
85748 Garching b. München
Telefon +49 89 32004-0
Telefax +49 89 32004-300

Kurfürstendamm 200
10719 Berlin
Telefon +49 30 88589-0
Telefax +49 30 88589-111

Theodor-Heuss-Straße 4
38122 Braunschweig
Telefon +49 531 8012-0
Telefax +49 531 8012-200

www.grs.de

ISBN 978-3-911727-38-9